Repetitive Spreading Depolarization induces gene expression changes related to synaptic plasticity and neuroprotective pathways.

Michela Dell'Orco [1], Jordan E. Weisend [1], Nora I. Perrone-Bizzozero [1], Andrew P. Carlson [2], Russell A. Morton [1], David N Linsenbardt [1] & C. William Shuttleworth [1]

[1]Department of Neurosciences, University of New Mexico School of Medicine, Albuquerque, New Mexico, 87131, USA.

[2]Department of Neurosurgery, University of New Mexico School of Medicine, Albuquerque, New Mexico, 87131, USA.

*** Correspondence:**
C. William Shuttleworth, Ph.D.
bshuttleworth@salud.unm.edu

Keywords: spreading depression, preconditioning, gene expression, pathway analysis, brain injury, stroke

Abstract

Spreading depolarization (SD) is a slowly propagating wave of profound depolarization that sweeps through cortical tissue. While much emphasis has been placed on the damaging consequences of SD, there is uncertainty surrounding the potential activation of beneficial pathways such as cell survival and plasticity. The present study used unbiased assessments of gene expression to evaluate that compensatory and repair mechanisms could be recruited following SD, regardless of the induction method, which prior to this work had not been assessed. We also tested assumptions of appropriate controls and the spatial extent of expression changes that are important for *in vivo* SD models. SD clusters were induced with either KCl focal application or optogenetic stimulation in healthy mice. Cortical RNA was extracted and sequenced to identify differentially expressed genes (DEGs). SDs using both induction methods significantly upregulated 16 genes (versus sham animals) that included the cell proliferation-related genes FOS, JUN, and DUSP6, the plasticity-related genes ARC and HOMER1, and the inflammation-related genes PTGS2, EGR2, and NR4A1. The contralateral hemisphere is commonly used as control tissue for DEG studies, but its activity could be modified by near-global disruption of activity in the adjacent brain. We found 21 upregulated genes when comparing SD-involved cortex versus tissue from the contralateral hemisphere of the same animals. Interestingly, there was almost complete overlap (21/16) with the DEGs identified using sham controls. Neuronal activity also differs in SD initiation zones, where sustained global depolarization is required to initiate propagating events. We found that gene expression varied as a function of the distance from the SD initiation site, with greater expression differences observed in regions further away. Functional and pathway enrichment analyses identified axonogenesis, branching, neuritogenesis, and dendritic growth as significantly enriched in overlapping DEGs. Increased expression of SD-induced genes was also associated with predicted inhibition of pathways associated with cell death, and apoptosis. These results identify novel biological pathways that could be involved in plasticity and/or circuit modification in brain tissue impacted by SD. These results also identify novel functional targets that could be tested to determine potential roles in recovery and survival of peri-infarct tissues.

1 Introduction

Spreading Depolarization (SD) is a slowly propagating wave of extended depolarization that is followed by transient suppression of neural activity, first described by Leao (Leao, 1944). SD is implicated as a mechanism of migraine with aura (Charles and Brennan, 2009; Pietrobon and Moskowitz, 2014) and otherwise healthy brain is able to fully recover from SD (Nedergaard and Hansen, 1988). However, the long duration of depolarization (up to a minute or more) can lead to severe energy depletion (Lindquist and Shuttleworth, 2014; Dreier et al., 2017), particularly when coupled with neurovascular disruptions in ischemic brain (Dreier, 2011; Ayata and Lauritzen, 2015; Hartings et al., 2017b). In addition, transient extracellular glutamate surges caused by SD can be sufficient to cause neuronal injury in metabolically compromised brain tissue (Aiba et al., 2012; Hinzman et al., 2015). Recent work has identified SDs as contributors to tissue loss following stroke, trauma, and other acute brain injuries (Lauritzen et al., 2011; Dreier et al., 2017) and initial efforts have begun targeting SD in efforts to improve outcomes in brain injury (Carlson et al., 2018; Helbok et al., 2020).

In contrast to the large body of literature characterizing electrophysiological and vascular responses to SD, only a relatively small number of studies have examined SD-induced gene expression changes and their relationship to outcomes in different experimental and clinical conditions (Urbach et al., 2006; Sintas et al., 2017). Initial studies identified increases in brain derived neurotrophic factor (BDNF), c-Fos and heat shock protein 70 (HSP70) (Kokaia et al., 1993; Matsushima et al., 1996; Karikó et al., 1998; Dietrich et al., 2000; Rangel et al., 2001). Subsequent studies showed increased expression of pro-inflammatory and apoptotic genes, including tumor necrosis factor (TNF), C-C motif chemokine ligand 2 (CCL2), interleukin-1 (IL-1) and -6, and cyclooxygenase-2 (COX-2), and B-cell lymphoma 2 (BCL-2) (Jander et al., 2001; Kaido et al., 2012; Eising et al., 2017; Takizawa et al., 2020). While most of these studies focused on a predetermined set of genes, a microarray study applied gene ontology (GO) and pathway analysis (PA) to examine the effect of SDs in rats (Sintas et al., 2017). This study identified upregulation of genes in pathways linked to oxidative stress and cellular injury, but less is known of other cellular adaptations that may occur. A lack of comprehensive transcriptomic analysis has limited the understanding of potentially beneficial pathways that could be activated following SD.

In the current study, we provide the first unbiased RNAseq analysis following SD. To increase generalizability, we combined data from the two most common methods of SD initiation (focal depolarization with either topical KCl administration or optogenetic stimulation) and generated clusters of SDs that are analogous to patterns of SDs that have been recorded from injured human brain. We also examined two key issues specific this type of study in SD models; 1) appropriate control tissues and 2) relative contribution of initiation and propagation sites to gene expression changes. Finally, we applied pathway analysis approaches to uncover candidate networks and novel genes altered by SD. The results identify the upregulation of multiple molecular pathways in the propagation zones of SD that could regulate potentially beneficial effects, such as neuritogenesis and synaptic plasticity.

2 Materials and Methods

2.1 Animal model

All experimental procedures were performed in accordance with the National Institutes of Health Guide for Care and Use of Laboratory Animals and were approved by the University of New Mexico Health Sciences Center Institutional Animal Care and Use Committee (IACUC). SDs were induced repetitively (4 SDs in 2 hours at 30 min intervals) in healthy 7-8-week-old female mice and SDs were confirmed with intrinsic optical signal imaging (Video 1, 2, and Supplementary Figure 1). SDs were

This is a provisional file, not the final typeset article

induced in 6 mice with either focal application of KCl through a burr hole in C57Bl6J mice (n=3) or with optogenetic stimulation (3 mW for 20 seconds) in Thy1-ChR2-YFP positive mice (n=3). Thy1-ChR2-YFP breeders were initially purchased from The Jackson Laboratory (B6.Cg-Tg(Thy1-COP4/EYFP)18Gfng/J, Strain #:007612, RRID:IMSR_JAX:007612) and crossed to maintain the line, as previously described (Arenkiel et al., 2007). With either stimulus, evoked SDs propagated throughout the neocortex ipsilateral to the stimulus, without crossing to the contralateral hemisphere **(Supplementary Figure 1, Video 1 and 2).** A matched number of sham controls was used with focal NaCl administration through a burrhole, in C57Bl/6 mice (n=3), or 0.4 mW for 20 seconds in Thy1-ChR2-YFP positive mice (n=3). Thirty minutes after the last SD, the anesthetized animal was decapitated and the brain extracted, washed with ice cold PBS and kept on ice.

2.2 RNA extraction and qRT-PCR validation

The contralateral and ipsilateral cortices were rapidly dissected from underlying striatum and the hippocampus and total RNA was extracted using TRIzol (Invitrogen, ThermoFisher, Waltham, MA. USA). Extractions were either from intact ipsilateral or contralateral cortices (Figures 2-7) or from regions ~18 mm^2 rapidly micro-dissected on ice (Figure 6). Where indicated, microdissections were made from 3 different regions of the ipsilateral hemisphere: 1) SD initiation site; 2) intermediate site > 3mm from initiation, 3) remote site >5 mm from initiation (Supplementary Figure 3). All collected tissues were then flash frozen and kept at –80°C until RNA extraction. RNA was quantified using Qubit (Bio-Rad) and its quality was determined using a NanoDrop 1000 (ThermoFisher), using absorbance at 260, 280 and 230 nm. Aliquots of 2 µg RNA were sent to Arraystar, Inc. for Illumina paired-end RNAseq as described below. To validate gene expression from our RNAseq data set, separate aliquots containing 1 µg of total RNA were reverse transcribed using SuperScript II reverse transcriptase (Life Technologies) following the manufacturer's protocol and qPCR carried out with a CFX96 Touch Real-Time PCR Detection System using SYBR Green mix (Life Technologies). Primer sequences for qRT-PCR for mouse mRNAs were obtained from PrimerBank (https://pga.mgh.harvard.edu/primerbank/). The GAPDH gene (FW TGTGATGGGTGTGAACCACGAGAA, RV GAGCCCTTCCACAATGCCAAAGTT) was used to normalize values. As shown in Supplementary Figure 3, GAPDH expression itself was unchanged by SD with either KCl or optogenetic induction of SD. The relative expression of target genes was determined using the comparative $2^{-\Delta Ct}$ method (Livak and Schmittgen, 2001).

Values were expressed as means ± SEM. Statistical analysis was performed using GraphPad Prism version 9 (La Jolla, CA, USA). The data were analyzed by unpaired t-test followed by Welch's correction or analysis of variance (ANOVA) followed by Dunnett's Multiple Comparison tests. Differences were considered statistically significant when p values were < 0.05 (*$p<0.05$, **$p<0.01$, ***$p<0.001$).

2.3 RNA sequencing

RNAseq analysis was performed by Arraystar Inc. (Rockville, MD). Total RNA (2 µg) was used to prepare the sequencing library in the following steps: total RNA was enriched by oligo (dT) magnetic beads (rRNA removed); RNAseq library was prepared using KAPA Stranded RNASeq Library Prep Kit (Illumina), which incorporates dUTP into the second cDNA strand and renders the RNAseq library strand-specific. The completed libraries were qualified with an Agilent 2100 Bioanalyzer and quantified by using the absolute quantification qPCR method. To sequence the libraries on an Illumina NovaSeq 6000 instrument, the barcoded libraries were mixed, denatured to single stranded DNA in NaOH, captured on Illumina flow cell, amplified *in situ,* and subsequently sequenced for 150 cycles for both ends on an Illumina NovaSeq 6000 instrument. Sequence quality was examined using the

128 FastQC software. The trimmed reads (trimmed 5', 3'-adaptor bases using cutadapt) were aligned to a
129 reference genome (Mouse genome GRCm38) using Hisat2 software.
130

131 **2.4 Differential expression analysis**

132 The expression levels of known genes and transcripts were calculated using the StringTie and Ballgown
133 software package (Pertea et al., 2016) and expressed as fragments per kilobase of transcript per million
134 mapped reads (FPKM). The number of identified genes and transcripts per group was calculated based
135 on the mean of FPKM in group > 0.5. Differentially expressed gene (DEG) and transcript analyses
136 were performed using an unpaired t-test followed by Welch's correction; a fold change (FC) threshold
137 of 1.25 and p value < 0.05 were used together to classify genes and transcripts as differentially
138 expressed. We subsequently performed DESeq2 analysis (Ge et al., 2018) with a false discovery rate
139 (FDR) correction cutoff of 0.01 and FC >1.5.

140 **2.5 Ingenuity Pathway Analysis**

141 Predicted molecular functions and biological pathways enriched in genes differentially expressed after
142 SD were identified using Ingenuity Pathway software (IPA, Content version: 62089861 (Release Date:
143 2021-02-17), Qiagen, https://www.qiagenbioinformatics.com/products/ingenuity-pathway-analysis,
144 (Krämer et al., 2014)). The analysis was set to filter nervous system expressed genes only; reference
145 set: Ingenuity Knowledge Base (Genes Only); and including direct and indirect relationships.

146

147 **3 Results**

148 **3.1 Identification of gene expression induced by repetitive spreading depolarizations.**

149 Healthy female mice were subjected to multiple SDs (4 over a period of 2 hours) which were generated
150 to match clusters of SDs in clinical settings (Dreier et al., 2017) This procedure has previously been
151 shown to induce robust transcriptional changes (Urbach et al., 2006; Sintas et al., 2017; Takizawa et
152 al., 2020). Thirty minutes after the last SD or sham stimulus, the neocortex was removed, and RNA
153 extracted from tissue subjected to SD or shams for subsequent RNA sequencing (see Materials and
154 Methods and **Supplementary Figure 1**).

155 Both focal KCl and optogenetic stimulation are utilized in studies of SD in brain injury, and thus to
156 increase generalizability of this initial study of SD regulation of target genes, data from these two SD-
157 stimulation methods were combined for differential expression (DE) analysis. For the combined DE
158 analysis, we performed unpaired t-tests followed by Welch's correction on the mapped 12944 genes.
159 We identified 102 significantly differentially expressed genes (DEGs) **(Figure 1A, black, FC > 1.25,**
160 **p value <0.05, n=6, Supplementary Table 1).** We subsequently performed DESeq2 analysis (Ge et
161 al., 2018) and identified 16 genes that were also significant after false discovery rate correction (FDR
162 <0.01, FC>1.5) when comparing the SD group with the sham tissues (**Figure 1A, red, FDR <0.01, FC**
163 **>1.5, n=6, Supplementary Table 1)**.

164 Consistent with previous studies (Kokaia et al., 1993; Dietrich et al., 2000; Rangel et al., 2001; Kaido
165 et al., 2012), we found significant changes in immediate early genes ARC, FOS and JUN proto-
166 oncogenes, and early growth response (EGR) genes. Other DEGs with significantly increased levels
167 included adrenoceptor beta 1 (ADRB1), dual specificity phosphatase (DUSP) gene family, the nuclear

This is a provisional file, not the final typeset article

168 receptor subfamily 4 group A member 1 (NR4A1), and prostaglandin-endoperoxide synthase 2
169 (PTGS2)

170 **3.2 Molecular networks regulated by repetitive SDs.**

171 We next used Ingenuity Pathway Analysis (IPA) to identify molecular networks and biological
172 pathways regulated by DEGs. This information was then used to obtain a prediction of physiological
173 and pathological brain processes altered by SD. Enriched pathway analysis on FDR significant genes
174 showed that genes upregulated by SD are involved in nervous system development and function, tissue
175 morphology and development. We also found significant enrichment in genes involved in cell death
176 and survival and cell morphology (**Supplemenraty Table 2**)

177 To achieve a more extensive enrichment analysis we then expanded IPA pathway analysis to genes
178 with p value< 0.05 and FC> 1.25. **Figure 1B** and **C** show the top two scored networks (score 63 and
179 35) generated by IPA with the combined DEGs upregulated in the SD group as compared to sham
180 animals. The intensity of the color red for each molecule is proportional to the fold change (FC) of the
181 labeled gene. Genes with FDR< 0.01 are also highlighted with thicker red outlines. Full arrows indicate
182 a direct relationship between molecules, while dotted arrows indicate a predicted indirect relationship.
183 Orange arrows and molecules indicate the predicted activation of a gene, while yellow indicates
184 predicted inhibition. These networks implicated SD target genes associated with cell proliferation and
185 synaptic activity, including cAMP responsive element binding protein 1 (CREB1), mitogen-activated
186 protein kinase 1 and 3 (MAPK1 and MAPK3), and HOMER1 (**Figure 1C**).

187 Predictions of SD-induced changes associated with known disease states and functions are shown in
188 **Table 1** and they include: neurological diseases, psychological disorders, nervous system development
189 and function, tissue morphology, and tissue development. The complete list of diseases and functions
190 and the genes associated with each pathway are reported in **Supplementary Table 2**. **Figure 1D** also
191 shows the number of genes associated with each pathway and associated p value range. They are shown
192 together so that different strengths of the network elements can be compared. A complete list of
193 networks and associated DEGs is reported in **Supplementary Table 3.**

194 **Figure 2** illustrates pathways related to cellular functions induced by repetitive spreading
195 depolarization. The top common pathways identified include: cellular assembly and organization,
196 cellular function and maintenance, and cellular development and proliferation (**Supplementary Table**
197 **4**). The heatmaps in **Figure 2A and B** show the p value and the activation z score for each pathway,
198 and a graphical representation of the cellular functions and genes involved, respectively. As shown in
199 **Figure 2**, each gene expression FC is proportional to their color intensity; orange arrows and pathways
200 indicate a predicted activation, whereas blue indicates increased levels of genes which lead to inhibition
201 of the pathway; genes with FDR< 0.01 are also highlighted with thicker red outlines. IPA analysis
202 predicted an activation of axonogenesis, axon branching, dendritic growth and branching and growth
203 of neurites, based on increased levels of genes such as VGF, FOS, PTGS2, JUN, BDNF, gamma-
204 aminobutyric acid type A receptor subunit beta3 (GABRB3), activating transcription factor 3 (ATF3),
205 and cyclin dependent kinase like 3 (CDKL3). We also found predicted activation of pathways
206 regulating neuronal development, long-term potentiation, and neurotransmission due to increased
207 expression of genes such as FOS, PTGS2, EGR2, BDNF, JUN, KCNJ2, ARC, and HOMER1.

208 Interestingly, we also found predicted inhibition of neuronal cell death (z score -0.903), apoptosis (z
209 score -1.197) (**Figure 2A**), together with increased development of neurons (z score +2.224) survival
210 of cerebral cortex cells (z score +1.774), and cell viability (z score +1.413) (**Figure 2B**), due to

211 increased expression of genes such as FOS, BDNF, ATF3, JUNB, DUSP1, neuronal PAS domain
212 protein 4 (NPAS4), nuclear factor interleukin 3 regulated (NFIL3), and SERPINE1.

213 3.3 Comparison between contralateral and ipsilateral hemispheres.

214 Many studies utilize the contralateral neocortex as a convenient comparison tissue for DEG studies
215 (Shen and Gundlach, 1998; Volobueva et al., 2023), as SD does not directly propagate across the corpus
216 collosum. However, even if SD does not directly propagate through the contralateral cortex, the
217 profound and widespread disruption of neuronal network activity produced by SD might be expected
218 to have some impact on neuronal activity and gene expression in the contralateral hemisphere. The
219 assumption that contralateral tissue is equivalent to tissue from sham animals for DE analysis has not
220 previously been tested.

221 We first performed DE analysis between these 2 tissues (i.e., contralateral hemispheres in animals
222 exposed to SD in the ipsilateral hemisphere vs. sham tissues). As shown in **Supplementary Figure 2**
223 only 9 genes were significantly differently expressed after unpaired t-test followed by Welch's
224 correction, but none of were still significant after FDR correction, confirming a high degree of
225 similarity between gene expression in these tissues.

226 We next performed the same analyses described above (**Figure 1**), but comparing tissue exposed to
227 repetitive SDs with the contralateral cortex in the same animals, rather than sham animals. Of the 12893
228 mapped genes 149 were significant after unpaired t-test followed by Welch's correction (**Figure 3A**,
229 black, FC >1.25, p value <0.05, n=6, **Supplementary Table 1**), of these 21 were also significant after
230 FDR correction (FDR <0.01, FC>1.5, n=6) (**Figure 3A**, red). IPA analysis confirmed a high similarity
231 between the sham and contralateral cortex when used as control compared to the SD group. **Figure**
232 **3B** and 3C show the top scored networks generated from the SD vs contralateral DEGs list, genes with
233 FDR< 0.01 are also highlighted with thicker red outlines. The top diseases and function are reported
234 in **Table 2** and Supplementary Table 2 (compare with Figure 1). Likewise, **Figure 4** shows cellular
235 and molecular pathways that are comparable with DEG analysis with sham tissues (compared with
236 **Figure 2**). These results imply that, at least at the level of gene expression changes after 2 hours, the
237 contralateral hemisphere that is not directly invaded by SD can likely serve as an unaffected control.

238 3.4 SD target genes control cell differentiation and proliferation, synaptic plasticity, and stress
239 responses.

240 To validate the predicted activation of neuroprotective pathways, we analyzed the expression levels of
241 a subset of SD target genes by qRT-PCR. The genes selected for validation where based on the IPA
242 analysis; indeed, enrichment pathways analysis was used to identify genes functionally related to SD
243 target genes that were not found significant in DE analysis. Based on the IPA results above, we focused
244 on genes regulating 3 cellular functions: 1) cell differentiation and proliferation, 2) synaptic plasticity
245 and 3) stress responses. qPCR was performed on the same RNA that was subjected to the RNAseq
246 analyses, as well as 3 additional animals for each group. As shown in **Figure 5**, multiple SDs resulted
247 in significant increases in the expression of genes activating cell proliferation and differentiation such
248 as BNDF, DUPS6, FOS and JUNB (**Figure 5**). Considering the predicted activation of neurons and
249 long-term potentiation, as well the increased axonogenesis, growth of neurites, and axon and neurites
250 branching, we then analyzed the expression of genes known for their regulation of synaptic plasticity.
251 As shown in **Figure 5** we found significantly increased expression of Homer1a and ARC. Finally, we
252 examined levels of PTGS2, NR4A1, and EGR2 as genes regulating stress and inflammatory responses,
253 showing a significant upregulation.

This is a provisional file, not the final typeset article

3.5 Target genes showed differential expression depending on the distance from the SD initiation site.

Lastly, we tested whether the levels of gene expression varied with distance from the SD initiation site. In this set of studies, KCl was used as the stimulus, as the site of initiation is clearly restricted to small zone of the application of KCl through the burr hole. Thus, two hours after onset of the initial SD, RNA was extracted from either total contralateral cortex, or from 3 different regions of the ipsilateral hemisphere: 1) SD initiation site; 2) intermediate site, and 3) remote site (see Methods and **Supplementary Figure 3**). By qRT-PCR we analyzed the levels of the previously identified target genes (see section 3 above) and compared these to the levels in the contralateral hemisphere of SHAM animals. For the majority of the genes examined (BDNF, DUSP6, PTGS2 ARC, and Homer 1a), highest expression was detected in the intermediate area (>3mm from the initiation site; **Figure 6**) while FOS and JUNB genes showed significantly increased expression in the remote site (>6 mm from the initiation site). Interestingly, when analyzing Homer1a levels, we found a decrease in their expression at the SD initiation site (**Figure 6**) when compared to the contralateral and intermediate sites (**Figure 6**). The difference between the contralateral and remote sites for NR4A1 did not reach statistical significance (p value=0.09) and EGR2 did not show differential expression across regions (**Supplementary Figure 3**).

4 Discussion

This study is the first unbiased analysis of whole transcriptome changes in healthy brain tissue following repetitive spreading depolarization (SD). The main findings are that SD produces a spectrum of gene expression changes that are more diverse than previously thought and which, based on enrichment pathway analysis, likely include multiple molecular networks that promote neuronal survival, recovery and repair. The expression changes were most prominent in areas of SD propagation, implying that it is the depolarization wave itself that produces the changes rather than areas involved in SD initiation. We also show that the contralateral hemisphere, which is not directly involved in the SD, can serve as a good control tissue for DE analyses, even though changes in functional connectivity likely occur during repetitive SD waves. Our findings provide a basis for more consideration of a wider and novel range of consequences of SD, in addition to the well-studied acute functional disruption or damage to injured tissues.

SD is a profound activation of brain tissue that leads to depolarization in the order of minutes, and cellular loading of Na^+, Ca^{2+} (Somjen, 2001; Hartings et al., 2017a), and activation of transcription factors (Ikeda et al., 1994; Sosthenes et al., 2019). In our study we confirmed that expression of immediate early genes is strongly upregulated, including that of established markers of neuronal activity such as FOS, JUNB and ARC (Ikeda et al., 1994; Hermann et al., 1999). SD is a global event that appears to involve all neurons and glia in its path (Somjen, 2001), and thus these markers of neuronal activation are expected to be uniformly activated in these cell types after SDs.

While RNAseq is a powerful tool for identifying genome-wide transcriptional alterations, standard differential gene expression analyses do not themselves leverage known biological gene network relationships. Using enrichment pathway analysis tools, we identified several additional key SD-activated molecules inferred as participants in larger functional networks. .
Increases in BDNF expression are among the most studied and strongly implicated in ischemic preconditioning and potentially plasticity after SD. BDNF increases were seen here as well. Consistent with previous work (Kokaia et al., 1993; Matsushima et al., 1998; Rangel et al., 2001; Yanamoto et al.,

298 2004), BDNF was one of the genes significantly increased by both KCl and optogenetic stimuli (**Figure**
299 **5 and 6**) and was identified in SD-induced pathways related to neuronal differentiation: neuritogenesis,
300 branching of axon sand neurites, and development of neurons (**Figure 2 and 4**). A surprising finding
301 was the extent of predicted pathways involved in neuronal plasticity and regeneration. For example
302 ARC mediates AMPA receptor endocytosis and is required for protein synthesis dependent LTP and
303 memory formation (Chowdhury et al., 2006). Similarly, Homer1 scaffolding protein controls the
304 insertion of postsynaptic glutamate receptors (Ango et al., 2002; Luo et al., 2012). Homer1a is
305 increased by synaptic activity through the MAP kinase pathway. This type of regulation creates a
306 negative feedback loop in which Homer1a inhibits Homer1b/c ability to scaffold and diminishes
307 synaptic strength by modulation of dendritic spine morphology and AMPA/NMDA receptor activity
308 (Sato et al., 2001; Bottai et al., 2002). This loop has been associated with TBI and epilepsy, particularly,
309 and is thought to block postsynaptic Ca^{2+}-mediated excitotoxicity (Cavarsan et al., 2012; Luo et al.,
310 2014). Consistent with these observations, prior work in brain slices and rodent cortex has reported
311 LTP-like synaptic strengthening following SD (Footitt and Newberry, 1998; Berger et al., 2008). In
312 addition previous studies have shown that SD leads to synaptic strengthening (Footitt and Newberry,
313 1998; Berger et al., 2008; Theriot et al., 2012) as well as adult neurogenesis (Urbach et al., 2017) and
314 preconditioning (Matsushima et al., 1998; Yanamoto et al., 2004; Shen et al., 2016). It will be of
315 interest to determine whether the time course of associated gene expression changes correspond to
316 variations in physiological recordings and how the expression of these genes change under different
317 metabolic conditions surrounding ischemic infarcts.

318 Consistent with previous reports, either from gene array studies or targeted expression analysis,
319 markers of inflammation were also upregulated (Urbach et al., 2006; Sintas et al., 2017). For example,
320 our results are consistent with prior reports of robust increases of the pro-inflammatory mediator COX2
321 (Kaido et al., 2012; Takizawa et al., 2020; Volobueva et al., 2023). We did not see significant increases
322 in some other inflammatory mediators that had been previously reported (e.g., TNF-α, IL-1β, IL6),
323 perhaps because the time course for peak increases in these mediators is later than the 2-hour time point
324 used in the present study (Takizawa et al., 2020). This time point was chosen based on 1) prior
325 expression analysis confirming peak increases at 2 hours for most genes of interest (Kokaia et al., 1993;
326 Karikó et al., 1998; Rangel et al., 2001) and 2) clinical recordings establishing clusters of SDs (usually
327 defined as three or more events within 2 hours) as being clinically significant (Dreier et al., 2006;
328 Hartings et al., 2020). Prior work (Takizawa et al., 2020) has shown that some inflammatory mediators
329 can be detected following a single SD (measured at 1 hour), while others peak at 24 h (Matsushima et
330 al., 1998; Jander et al., 2001; Volobueva et al., 2023). It remains to be determined which of the genes
331 seen here may peak earlier or at later times points.

332 A second surprising finding came from pathway analysis of genes associated with neuronal injury or
333 apoptotic cell death. The pathways analysis indicated a downregulation of these pathways, based on
334 differential expression of molecular components of cell viability or apoptotic pathways such as: BDNF,
335 FOS, EGR1 and 2, ATF3, NAPS4, CXCL2, and MAPKs (**Figure 2 and 4**). This raises the possibility
336 that the extreme metabolic challenge of SD may be capable of promoting cell survival by decreasing
337 cell death pathways. This does not mean that SDs are not causing neuronal injury – it means instead
338 that SD is likely able to kill neurons due to extreme metabolic depletion, but in neurons that are able
339 to recover from that acute insult, gene expression changes favor survival, including downregulation of
340 cell death pathways. While further studies will be required to test if SDs is sufficient for a positive
341 outcome after stroke or brain injury; this work shows that in tissues with sufficient perfusion, SD itself
342 can induce the expression of neuroprotective pathways.

This is a provisional file, not the final typeset article

Another important experimental consideration that is somewhat unique for SD studies, is the choice of control tissue. SDs can propagate throughout a hemisphere but generally do not cross the midline and invade the contralateral hemisphere. For this reason, the contralateral hemisphere is often used as a control tissue for DEG studies (Shen and Gundlach, 1998; Wiggins et al., 2003; Volobueva et al., 2023), with the assumption that it is unaffected by SD. However, a well-established consequence of SD is a spreading depression of synaptic transmission throughout the affected cortex and, because of the connectivity between hemispheres (Leao, 1944; Vinogradova et al., 2021), an abrupt silencing of such large territory is expected to have consequences on circuit activity throughout the brain. We therefore tested whether the results of DEG analysis were different if the contralateral hemisphere was used instead of different animals in which no SD was generated (shams, as used in **Figures 3 and 4**). Interestingly, there was a very similar (although not identical) set of DEGs in both control tissues, implying differences in connectivity only cause minor differences in expression in the contralateral hemisphere compared with the changes produced by propagation of SD through the ipsilateral cortex. This suggests that the benefits of using control tissue from the same animal (to reduce inter-animal variability) may outweigh small changes in state for most SD studies.

Gene expression studies of SD have specific experimental challenges, related to the unusually extreme global disruptions produced by the events. Firstly, experimentally-induced SDs require coordinated depolarization of a volume of brain tissue that can be accomplished by a range of methods. Two commonly used methods (focal application of KCl and optogenetic stimulation) of SD were used here and combined, to increase generalizability of results. We then tested whether a microdissection and qPCR would show differences in propagation areas, as compared with the initiation sites. Interestingly, the largest expression changes were observed in the propagation regions (**Figure 6**), despite the fact that depolarization may be most intense at the initiation site. Factors released by SD or intracellular pathways activated by the combination of factors released at the wave front may be responsible. It also suggests that any injury or other damage produced at an initiation site was not the driver of changes observed in the study. Spatial genomics approaches (Ibarra-Lopez et al., 2022) will be useful to further investigate the distribution of changes of larger gene sets with distance from SD initiation, and with respect to differential vascular perfusion, for example.

In conclusion, these findings provide a basis for considering long-term changes due to SD that can influence outcomes in a range of neurological disorders. While SDs can clearly be damaging to vulnerable brain tissue, our work shows the changes in gene expression may also promote neuronal survival in some areas. If the predicted pathways involved in neuronal differentiation and growth are manifest in surviving peri-infarct tissues, for example, then there may be benefit to preserving these effects while preventing deleterious consequences of SD. These results also emphasize the importance of experimental design for SD studies. Finally, SDs that are experimentally generated outside a zone of vulnerable tissue may have the ability to activate pro-survival pathways predicted in the current study and thereby contribute to apparent paradoxical results in experimental models of stroke. Further studies will be essential to determine whether SD induction of neuronal survival pathways are sufficient to improve recovery and outcomes in stroke and brain injury.

5 Data Availability Statement

The data presented in this publication have been deposited in NCBI's Gene Expression Omnibus (Edgar et al., 2002) and are accessible through GEO Series accession number GSE214623 (https://www.ncbi.nlm.nih.gov/geo/query/acc.cgi?acc=GSE214623).

6 Conflict of Interest

The authors declare that the research was conducted in the absence of any commercial or financial relationships that could be construed as a potential conflict of interest.

7 Author Contributions

MD designed and performed the experiments, analysed the data, and wrote the manuscript together with JW, NPB, RM and DL. CWS supervised the project and was in charge of the overall planning and data analysis. All authors discussed the results and contributed to the final manuscript.

8 Funding

This work was supported by the National Institute of Health grants NS106901 and P206GM109089.

9 Acknowledgments

We thank the Animal Research Facility (ARF) of the Health Science Center (HSC), University of New Mexico School of Medicine. We also thank the UNM Preclinical Core of the Center from Brain Recovery and Repair (University of New Mexico) for technical support.

10 Ethics Statement

The animal study was reviewed and approved by the University of New Mexico Health Sciences Center Institutional Animal Care and Use Committee.

11 References

Aiba, I., Carlson, A. P., Sheline, C. T., and William, S. C. (2012). Synaptic release and extracellular actions of zn 2+ limit propagation of spreading depression and related events in vitro and in vivo. *J. Neurophysiol.* 107, 1032–1041. doi: 10.1152/jn.00453.2011.

Ango, F., Robbe, D., Tu, J. C., Xiao, B., Worley, P. F., Pin, J.-P., et al. (2002). Homer-dependent cell surface expression of metabotropic glutamate receptor type 5 in neurons. *Mol. Cell. Neurosci.* 20, 323–9. Available at: http://www.ncbi.nlm.nih.gov/pubmed/12093163 [Accessed August 13, 2019].

Arenkiel, B. R., Peca, J., Davison, I. G., Feliciano, C., Deisseroth, K., Augustine, G. J. J., et al. (2007). In vivo light-induced activation of neural circuitry in transgenic mice expressing channelrhodopsin-2. *Neuron* 54, 205–218. doi: 10.1016/J.NEURON.2007.03.005.

This is a provisional file, not the final typeset article

418 Ayata, C., and Lauritzen, M. (2015). Spreading Depression, Spreading Depolarizations, and the
419 Cerebral Vasculature. *Physiol. Rev.* 95, 953–993. doi: 10.1152/PHYSREV.00027.2014.

420 Berger, M., Speckmann, E. J., Pape, H. C., and Gorji, A. (2008). Spreading depression enhances
421 human neocortical excitability in vitro. *Cephalalgia* 28, 558–562. doi: 10.1111/J.1468-
422 2982.2008.01556.X.

423 Bottai, D., Guzowski, J. F., Schwarz, M. K., Kang, S. H., Xiao, B., Lanahan, A., et al. (2002).
424 Synaptic Activity-Induced Conversion of Intronic to Exonic Sequence in Homer 1 Immediate
425 Early Gene Expression. *J. Neurosci.* 22, 167. doi: 10.1523/JNEUROSCI.22-01-00167.2002.

426 Carlson, A. P., Abbas, M., Alunday, R. L., Qeadan, F., and William Shuttleworth, C. (2018).
427 Spreading depolarization in acute brain injury inhibited by ketamine: a prospective, randomized,
428 multiple crossover trial. *J. Neurosurg.* 130, 1513–1519. doi: 10.3171/2017.12.JNS171665.

429 Cavarsan, C. F., Tescarollo, F., Tesone-Coelho, C., Morais, R. L. T., Motta, F. L. T., Blanco, M. M.,
430 et al. (2012). Pilocarpine-induced status epilepticus increases Homer1a and changes mGluR5
431 expression. *Epilepsy Res.* 101, 253–260. doi: 10.1016/J.EPLEPSYRES.2012.04.011.

432 Charles, A., and Brennan, K. C. (2009). Cortical spreading depression-new insights and persistent
433 questions. *Cephalalgia* 29, 1115–1124. doi: 10.1111/J.1468-2982.2009.01983.X.

434 Chowdhury, S., Shepherd, J. D., Okuno, H., Lyford, G., Petralia, R. S., Plath, N., et al. (2006). Arc
435 Interacts with the Endocytic Machinery to Regulate AMPA Receptor Trafficking. *Neuron* 52,
436 445. doi: 10.1016/J.NEURON.2006.08.033.

437 Dietrich, W. D., Truettner, J., Prado, R., Stagliano, N. E., Zhao, W., Busto, R., et al. (2000).
438 Thromboembolic events lead to cortical spreading depression and expression of c-fos, brain-
439 derived neurotrophic factor, glial fibrillary acidic protein, and heat shock protein 70 mRNA in
440 rats. *J. Cereb. Blood Flow Metab.* 20, 103–11. doi: 10.1097/00004647-200001000-00014.

441 Dreier, J. P. (2011). The role of spreading depression, spreading depolarization and spreading
442 ischemia in neurological disease. *Nat. Med.* 17, 439–447. doi: 10.1038/nm.2333.

443 Dreier, J. P., Fabricius, M., Ayata, C., Sakowitz, O. W., William Shuttleworth, C., Dohmen, C., et al.
444 (2017). Recording, analysis, and interpretation of spreading depolarizations in neurointensive
445 care: Review and recommendations of the COSBID research group. *J. Cereb. Blood Flow*
446 *Metab.* 37, 1595–1625. doi: 10.1177/0271678X16654496.

447 Dreier, J. P., Woitzik, J., Fabricius, M., Bhatia, R., Major, S., Drenckhahn, C., et al. (2006). Delayed
448 ischaemic neurological deficits after subarachnoid haemorrhage are associated with clusters of
449 spreading depolarizations. *Brain* 129, 3224–3237. doi: 10.1093/BRAIN/AWL297.

450 Edgar, R., Domrachev, M., and Lash, A. E. (2002). Gene Expression Omnibus: NCBI gene
451 expression and hybridization array data repository. *Nucleic Acids Res.* 30, 207–210. doi:
452 10.1093/NAR/30.1.207.

453 Eising, E., Shyti, R., ’t Hoen, P. A. C., Vijfhuizen, L. S., Huisman, S. M. H., Broos, L. A. M., et al.
454 (2017). Cortical Spreading Depression Causes Unique Dysregulation of Inflammatory Pathways
455 in a Transgenic Mouse Model of Migraine. *Mol. Neurobiol.* 54, 2986–2996. doi:

456 10.1007/S12035-015-9681-5.

457 Footitt, D. R., and Newberry, N. R. (1998). Cortical spreading depression induces an LTP-like effect
458 in rat neocortex in vitro. *Brain Res.* 781, 339–342. doi: 10.1016/S0006-8993(97)01359-0.

459 Ge, S. X., Son, E. W., and Yao, R. (2018). iDEP: An integrated web application for differential
460 expression and pathway analysis of RNA-Seq data. *BMC Bioinformatics* 19, 1–24. doi:
461 10.1186/s12859-018-2486-6.

462 Hartings, J. A., Andaluz, N., Bullock, M. R., Hinzman, J. M., Mathern, B., Pahl, C., et al. (2020).
463 Prognostic Value of Spreading Depolarizations in Patients With Severe Traumatic Brain Injury.
464 *JAMA Neurol.* 77, 489–499. doi: 10.1001/JAMANEUROL.2019.4476.

465 Hartings, J. A., Li, C., Hinzman, J. M., Shuttleworth, C. W., Ernst, G. L., Dreier, J. P., et al. (2017a).
466 Direct current electrocorticography for clinical neuromonitoring of spreading depolarizations. *J.*
467 *Cereb. Blood Flow Metab.* 37, 1857–1870. doi: 10.1177/0271678X16653135.

468 Hartings, J. A., Shuttleworth, C. W., Kirov, S. A., Ayata, C., Hinzman, J. M., Foreman, B., et al.
469 (2017b). The continuum of spreading depolarizations in acute cortical lesion development:
470 Examining Leão's legacy. *J. Cereb. Blood Flow Metab.* 37, 1571–1594. doi:
471 10.1177/0271678X16654495.

472 Helbok, R., Hartings, J. A., Schiefecker, A., Balança, B., Jewel, S., Foreman, B., et al. (2020). What
473 Should a Clinician Do When Spreading Depolarizations are Observed in a Patient? *Neurocrit.*
474 *Care* 32, 306–310. doi: 10.1007/s12028-019-00777-6.

475 Hermann, D. M., Mies, G., and Hossmann, K. A. (1999). Expression of c-fos, junB, c-jun, MKP-1
476 and hsp72 following traumatic neocortical lesions in rats--relation to spreading depression.
477 *Neuroscience* 88, 599–608. doi: 10.1016/s0306-4522(98)00249-8.

478 Hinzman, J. M., DiNapoli, V. A., Mahoney, E. J., Gerhardt, G. A., and Hartings, J. A. (2015).
479 Spreading depolarizations mediate excitotoxicity in the development of acute cortical lesions.
480 *Exp. Neurol.* 267, 243–253. doi: 10.1016/j.expneurol.2015.03.014.

481 Ibarra-Lopez, V., Jayakar, S., Yang, Y. A., Martin, C., Modrusan, Z., and Rost, S. (2022). Spatial
482 Profiling of Protein and RNA Expression in Tissue: An Approach to Fine-tune Virtual
483 Microdissection. *J. Vis. Exp.* doi: 10.3791/62651.

484 Ikeda, J., Nakajima, T., Osborne, O. C., Mies, G., and Nowak, T. S. (1994). Coexpression of c-fos
485 and hsp70 mRNAs in gerbil brain after ischemia: Induction threshold, distribution and time
486 course evaluated by in situ hybridization. *Mol. Brain Res.* 26, 249–258. doi: 10.1016/0169-
487 328X(94)90097-3.

488 Jander, S., Schroeter, M., Peters, O., Witte, O. W., and Stoll, G. (2001). Cortical spreading
489 depression induces proinflammatory cytokine gene expression in the rat brain. *J. Cereb. Blood*
490 *Flow Metab.* 21, 218–225. doi: 10.1097/00004647-200103000-00005.

491 Kaido, Kempski, Heimann, Heers, and Bartsch (2012). Cluster analysis of mRNA expression levels
492 identifies multiple sequential patterns following focal cerebral ischemia. *Turk. Neurosurg.* 22.
493 doi: 10.5137/1019-5149.JTN.5523-11.0.

This is a provisional file, not the final typeset article

494 Karikó, K., Harris, V. A., Rangel, Y., Duvall, M. E., and Welsh, F. A. (1998). Effect of cortical
495 spreading depression on the levels of mRNA coding for putative neuroprotective proteins in rat
496 brain. *J. Cereb. Blood Flow Metab.* 18, 1308–1315. doi: 10.1097/00004647-199812000-00005.

497 Kokaia, Z., Gidö, G., Ringstedt, T., Bengzon, J., Kokaia, M., Siesjö, B. K., et al. (1993). Rapid
498 increase of BDNF mRNA levels in cortical neurons following spreading depression: regulation
499 by glutamatergic mechanisms independent of seizure activity. *Mol. Brain Res.* 19, 277–286. doi:
500 10.1016/0169-328X(93)90126-A.

501 Krämer, A., Green, J., Pollard, J., and Tugendreich, S. (2014). Causal analysis approaches in
502 Ingenuity Pathway Analysis. *Bioinformatics* 30, 523–530. doi:
503 10.1093/BIOINFORMATICS/BTT703.

504 Lauritzen, M., Dreier, J. P., Fabricius, M., Hartings, J. A., Graf, R., and Strong, A. J. (2011). Clinical
505 relevance of cortical spreading depression in neurological disorders: Migraine, malignant stroke,
506 subarachnoid and intracranial hemorrhage, and traumatic brain injury. *J. Cereb. Blood Flow*
507 *Metab.* 31, 17–35. doi: 10.1038/jcbfm.2010.191.

508 Leao, A. A. P. (1944). SPREADING DEPRESSION OF ACTIVITY IN THE CEREBRAL
509 CORTEX. *J. Neurophysiol.* 7, 359–390. doi: 10.1152/jn.1944.7.6.359.

510 Lindquist, B. E., and Shuttleworth, C. W. (2014). Spreading depolarization-induced adenosine
511 accumulation reflects metabolic status in vitro and in vivo. *J. Cereb. Blood Flow Metab.* 34,
512 1779–1790. doi: 10.1038/jcbfm.2014.146.

513 Livak, K. J., and Schmittgen, T. D. (2001). Analysis of relative gene expression data using real-time
514 quantitative PCR and the 2-ΔΔCT method. *Methods* 25, 402–408. doi: 10.1006/meth.2001.1262.

515 Luo, P., Chen, T., Zhao, Y., Zhang, L., Yang, Y., Liu, W., et al. (2014). Postsynaptic scaffold protein
516 Homer 1a protects against traumatic brain injury via regulating group I metabotropic glutamate
517 receptors. *Cell Death Dis.* 5. doi: 10.1038/CDDIS.2014.116.

518 Luo, P., Li, X., Fei, Z., and Poon, W. (2012). Scaffold protein Homer 1: Implications for neurological
519 diseases. *Neurochem. Int.* 61, 731–738. doi: 10.1016/j.neuint.2012.06.014.

520 Matsushima, K., Hogan, M. J., and Hakim, A. M. (1996). Cortical spreading depression protects
521 against subsequent focal cerebral ischemia in rats. *J. Cereb. Blood Flow Metab.* 16, 221–226.
522 doi: 10.1097/00004647-199603000-00006.

523 Matsushima, K., Schmidt-Kastner, R., Hogan, M. J., and Hakim, A. M. (1998). Cortical spreading
524 depression activates trophic factor expression in neurons and astrocytes and protects against
525 subsequent focal brain ischemia. *Brain Res.* 807, 47–60. doi: 10.1016/s0006-8993(98)00716-1.

526 Nedergaard, M., and Hansen, A. J. (1988). Spreading depression is not associated with neuronal
527 injury in the normal brain. *Brain Res.* 449, 395–398. doi: 10.1016/0006-8993(88)91062-1.

528 Pertea, M., Kim, D., Pertea, G. M., Leek, J. T., and Salzberg, S. L. (2016). Transcript-level
529 expression analysis of RNA-seq experiments with HISAT, StringTie and Ballgown. *Nat.*
530 *Protoc. 2016 119* 11, 1650–1667. doi: 10.1038/nprot.2016.095.

531 Pietrobon, D., and Moskowitz, M. A. (2014). Chaos and commotion in the wake of cortical spreading
532 depression and spreading depolarizations. *Nat. Rev. Neurosci.* 15, 379–393. doi:
533 10.1038/NRN3770.

534 Rangel, Y. M., Karikó, K., Harris, V. A., Duvall, M. E., and Welsh, F. A. (2001). Dose-dependent
535 induction of mRNAs encoding brain-derived neurotrophic factor and heat-shock protein-72 after
536 cortical spreading depression in the rat. *Mol. Brain Res.* 88, 103–112. doi: 10.1016/S0169-
537 328X(01)00037-7.

538 Sato, M., Suzuki, K., and Nakanishi, S. (2001). NMDA receptor stimulation and brain-derived
539 neurotrophic factor upregulate homer 1a mRNA via the mitogen-activated protein kinase
540 cascade in cultured cerebellar granule cells. *J. Neurosci.* 21, 3797–3805. doi:
541 10.1523/JNEUROSCI.21-11-03797.2001.

542 Shen, P. J., and Gundlach, A. L. (1998). Differential spatiotemporal alterations in adrenoceptor
543 mRNAs and binding sites in cerebral cortex following spreading depression: Selective and
544 prolonged up-regulation of α(1B)-adrenoceptors. *Exp. Neurol.* 154, 612–627. doi:
545 10.1006/exnr.1998.6915.

546 Shen, P. P., Hou, S., Ma, D., Zhao, M. M., Zhu, M. Q., Zhang, J. D., et al. (2016). Cortical spreading
547 depression-induced preconditioning in the brain. *Neural Regen. Res.* 11, 1857–1864. doi:
548 10.4103/1673-5374.194759.

549 Sintas, C., Fernàndez-Castillo, N., Vila-Pueyo, M., Pozo-Rosich, P., Macaya, A., and Cormand, B.
550 (2017). Transcriptomic Changes in Rat Cortex and Brainstem After Cortical Spreading
551 Depression With or Without Pretreatment With Migraine Prophylactic Drugs. *J. Pain* 18, 366–
552 375. doi: 10.1016/j.jpain.2016.11.007.

553 Somjen, G. G. (2001). Mechanisms of spreading depression and hypoxic spreading depression-like
554 depolarization. *Physiol. Rev.* 81, 1065–1096. doi: 10.1152/PHYSREV.2001.81.3.1065.

555 Sosthenes, M. C. K., Diniz, D. G., Roodselaar, J., Abadie-Guedes, R., de Siqueira Mendes, F. de C.
556 C., Fernandes, T. N., et al. (2019). Stereological Analysis of Early Gene Expression Using Egr-1
557 Immunolabeling After Spreading Depression in the Rat Somatosensory Cortex. *Front.*
558 *Neurosci.* 13, 1020. doi: 10.3389/fnins.2019.01020.

559 Takizawa, T., Qin, T., Morais, A. L. de, Sugimoto, K., Chung, J. Y., Morsett, L., et al. (2020). Non-
560 invasively triggered spreading depolarizations induce a rapidpro-inflammatory response in
561 cerebral cortex. *J. Cereb. Blood Flow Metab.* 40, 1117. doi: 10.1177/0271678X19859381.

562 Theriot, J. J., Toga, A. W., Prakash, N., Sungtaek Ju, Y., and Brennan, K. C. (2012). Cortical sensory
563 plasticity in a model of migraine with aura. *J. Neurosci.* 32, 15252–15261. doi:
564 10.1523/JNEUROSCI.2092-12.2012.

565 Urbach, A., Baum, E., Braun, F., and Witte, O. W. (2017). Cortical spreading depolarization
566 increases adult neurogenesis, and alters behavior and hippocampus-dependent memory in mice.
567 *J. Cereb. Blood Flow Metab.* 37, 1776–1790. doi: 10.1177/0271678X16643736.

568 Urbach, A., Bruehl, C., and Witte, O. W. (2006). Microarray-based long-term detection of genes
569 differentially expressed after cortical spreading depression. *Eur. J. Neurosci.* 24, 841–856. doi:

This is a provisional file, not the final typeset article

570 10.1111/j.1460-9568.2006.04862.x.

571 Vinogradova, L. V., Suleymanova, E. M., and Medvedeva, T. M. (2021). Transient loss of
572 interhemispheric functional connectivity following unilateral cortical spreading depression in
573 awake rats. *Cephalalgia* 41, 353–365. doi: 10.1177/0333102420970172.

574 Volobueva, M. N., Suleymanova, E. M., Smirnova, M. P., Bolshakov, A. P., and Vinogradova, L. V.
575 (2023). A Single Episode of Cortical Spreading Depolarization Increases mRNA Levels of
576 Proinflammatory Cytokines, Calcitonin Gene-Related Peptide and Pannexin-1 Channels in the
577 Cerebral Cortex. *Int. J. Mol. Sci.* 24. doi: 10.3390/ijms24010085.

578 Wiggins, A. K., Shen, P.-J. J., and Gundlach, A. L. (2003). Atrial natriuretic peptide expression is
579 increased in rat cerebral cortex following spreading depression: possible contribution to sd-
580 induced neuroprotection. *Neuroscience* 118, 715–726. doi: 10.1016/s0306-4522(03)00006-x.

581 Yanamoto, H., Xue, J. H., Miyamoto, S., Nagata, I., Nakano, Y., Murao, K., et al. (2004). Spreading
582 depression induces long-lasting brain protection against infarcted lesion development via BDNF
583 gene-dependent mechanism. *Brain Res.* 1019, 178–188. doi: 10.1016/j.brainres.2004.05.105.

584

585

586 **Figure Legends**

587 **Figure 1. Repetitive SD increases levels of genes related to nervous system development and**
588 **function A)** Differential Expression (DE) analysis. We performed unpaired t-test followed by Welch's
589 correction; significant genes (FC > 1.25, p value <0.05, n=6) are represented in black. Consequently,
590 we performed DESeq2 analysis (Ge, Son, and Yao 2018); genes that were also significant after false
591 discovery rate correction (FDR <0.01, n=6) are represented in red. **B) and C)** top molecular networks
592 (score 63 and 32) generated by IPA analysis of DEGs upregulated in SD animals vs sham. The intensity
593 of the color red for each molecule is proportional to the FC of the gene. Genes with FDR<0.01 are
594 highlighted with a thicker red outline. Full arrows indicate a direct relationship between molecules,
595 while dotted arrows indicate an indirect relationship between genes. Orange arrows and molecules
596 indicate the predicted activation of a gene, while yellow indicates predicted inhibition. **D)** Top diseases
597 and functions determined from the IPA analysis.

598 **Figure 2**. **Top cellular pathways activated by SD. A)** Neural death and survival pathways. **B)**
599 Cellular proliferation and growth. Top cellular functions generated by IPA analysis of DEGs
600 upregulated in SD animals vs sham. The heatmaps show the p value and the activation score for each
601 pathway. **A') and B')** Graphical representations of the networks and the genes involved in A and B.
602 The intensity of the color red for each molecule is proportional to the FC of the gene. Orange arrows
603 indicate a positive control of the gene on the related pathway, and the pathway's name highlighted in
604 orange indicates its activation. Genes with FDR< 0.01 are also highlighted with thicker red outlines.
605 Apoptosis z score -1.197, neuronal cell death z score -0.903, neuritogenesis z score +2.048, branching
606 of neurites z score +1.924, branching of axons z score +1.922, development of neurons z score +2.224.

607 **Figure 3. Sham animals and contralateral cortex are equivalent controls for unilateral SDs. A**)
608 Differential Expression (DE) analysis. We performed unpaired t-test followed by Welch's correction;
609 significant genes (FC > 1.25, p value <0.05, n=6) are represented in black. Subsequently, we performed

610 DESeq2 analysis (Ge, Son, and Yao 2018); genes that were also significant after false discovery rate
611 correction (FDR <0.01, n=6) are represented in red. **B**) top molecular networks (score 65 and 34)
612 generated by IPA analysis of DEGs upregulated in SD animals vs contralateral. The intensity of the
613 color red for each molecule is proportional to the FC of the gene. Full arrows indicate a direct
614 relationship between molecules, while dotted arrows indicate an indirect relationship between genes.
615 Orange arrows indicate the predicted activation of a gene, while yellow indicates predicted inhibition.
616 Genes with FDR< 0.01 are also highlighted with thicker red outlines. **C**) Top diseases and functions
617 determined from IPA analysis.

618 **Figure 4**. **Top Cellular functions generated by IPA analysis of DEGs upregulated in SD animals**
619 **vs Contralateral.** A) Neural death and survival pathways. B) Cellular proliferation and growth. Top
620 cellular functions generated by IPA analysis of DEGs upregulated in SD animals vs sham. The
621 heatmaps show the p value and the activation score for each pathway. A') and B') Graphical
622 representations of the networks and the genes involved in A and B. The intensity of the color red for
623 each molecule is proportional to the FC of the gene. Orange arrows indicate a positive control of the
624 gene on the related pathway, and the pathway's name highlighted in orange indicates its activation.
625 Genes with FDR< 0.01 are also highlighted with thicker red outlines. Apoptosis z score -2.003,
626 neuronal cell death z score -1.974, density of spines z score +1.165, branching of neurons z score
627 +1.913, dendritic growth/branching z score +1.090, and development of neurons z score +2.286.

628 **Figure 5**. **SD target genes control cell differentiation and proliferation, synaptic plasticity, and**
629 **stress responses.** RT-qPCR validation of SD target genes identified by RNAseq and enrichment
630 analysis. mRNA levels of the target genes were measured as described in Material and Methods. Data
631 were analyzed by unpaired t-test, followed by Welch's correction and are represented as mean ± SEM;
632 p<0.05*, **p<0.01, ***p<0.001; n=6.

633 **Figure 6**. **Target genes showed differential expression depending on the distance from the SD**
634 **initiation site.** mRNA levels of the target genes were measured as described in Material and Methods.
635 Specifically, we determined the mRNA levels in 4 different regions: 1) SD initiation site, 2) SD
636 intermediate site, 3) SD remote site, and 4) the contralateral hemisphere. Data were analyzed by 2-way
637 ANOVA followed by Tukey's Multiple Comparison test, and are represented as mean ± SEM;
638 p<0.05*, **p<0.01, ***p<0.001; and unpaired t-test, followed by Welch's correction and are
639 represented as mean ± SEM; #p<0.05, ##p<0.01, ###p<0.001; n=3.

640

641

This is a provisional file, not the final typeset article

642

Disease and Disorders	p-value range	# Molecules
Neurological Diseases	3.69E-02 - 7.77E-09	42
Organismal Injury and Abnormalities	3.69E-02 - 6.10E-09	43
Psychological Disorders	2.65E-02 - 6.10E-09	29
Hereditary Disorders	2.65E-02 - 6.10E-09	18
Skeletal and Muscular Disorders	2.65E-02 - 2.70E-08	17
Physiological System Development and Functions	**p-value range**	**# Molecules**
Nervous System Development and Function	3.69E-02 - 7.62E-07	51
Tissue Morphology	3.69E-02 - 4.54E-08	28
Tissue Development	3.46E-02 - 7.62E-07	40
Organismal Development	3.46E-02 - 4.43E-06	37
Behavior	3.17E-02 - 1.11E-05	12

643 **Table1.** Predictions of SD-induced changes in associated nervous system diseases and functions, in
644 SD vs Sham Animals.

645

Disease and Disorders	p-value range	# Molecules
Neurological Diseases	4.56E-02 - 2.49E-08	73
Organismal Injury and Abnormalities	4.56E-02 - 1.91E-08	73
Psychological Disorders	2.85E-02 - 1.91E-08	35
Hereditary Disorders	1.54E-02 - 1.91E-08	21
Skeletal and Muscular Disorders	7.75E-03 - 6.30E-08	20
Physiological System Development and Functions	**p-value range**	**# Molecules**
Nervous System Development and Function	4.56E-02 - 7.04E-07	61
Tissue Morphology	4.56E-02 - 1.07E-09	39
Tissue Development	4.56E-02 - 1.03E-06	49
Organismal Development	4.56E-02 - 5.03E-06	44
Organ Morphology	4.56E-02 - 5.96E-05	16

646 **Table 2.** Predictions of SD-induced changes associated nervous system disease states and functions,
647 in SD ipsilateral vs contralateral cortex.

648

649

This is a provisional file, not the final typeset article

1A.

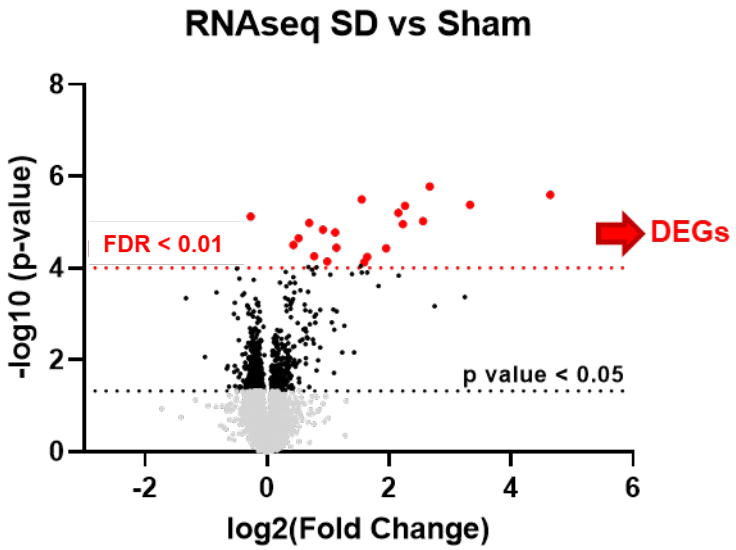

	log2 FC	Adj.Pval
NPAT	4.58	7.44E-04
PTGS2	3.32	1.38E-15
FOS	3.10	1.61E-12
EGR2	2.73	1.63E-04
FOSB	2.61	1.61E-12
ARC	2.50	6.13E-19
DUSP6	2.14	2.26E-08
JUNB	2.12	3.32E-15
DUSP5	2.05	3.45E-06
EGR4	1.97	4.92E-13
ARL4D	1.67	3.95E-15
RGS2	1.63	2.01E-06
GADD45G	1.58	3.22E-10
BTG2	1.57	1.90E-04
DUSP1	1.55	2.81E-07
EGR1	1.52	3.02E-12

Fold Change

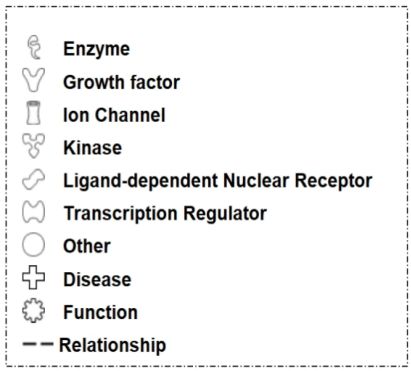

1B.

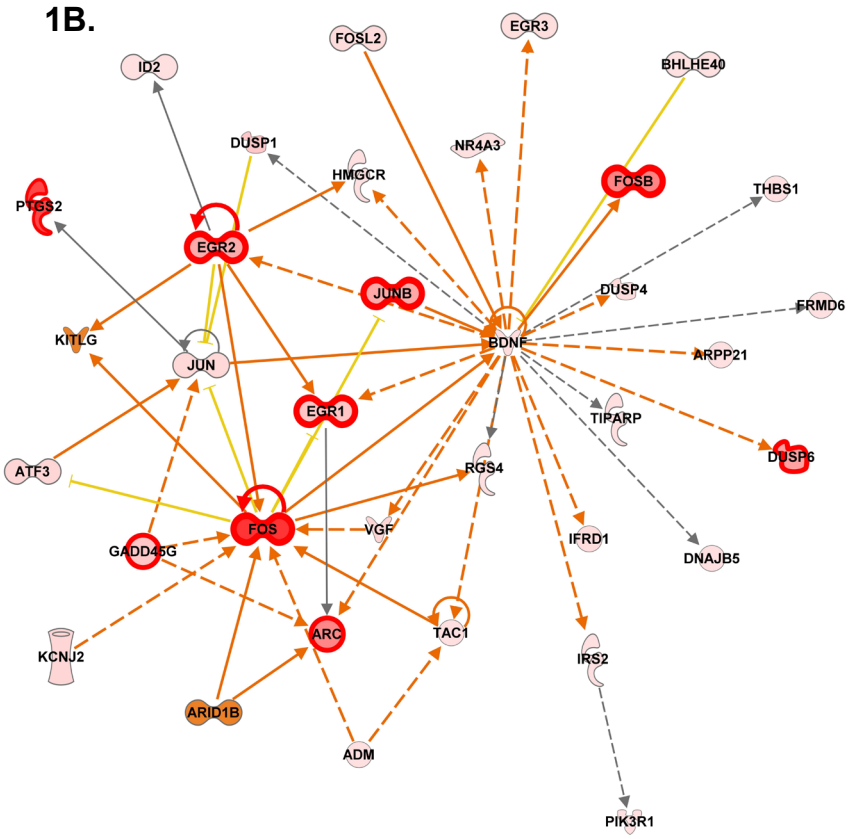

1C.

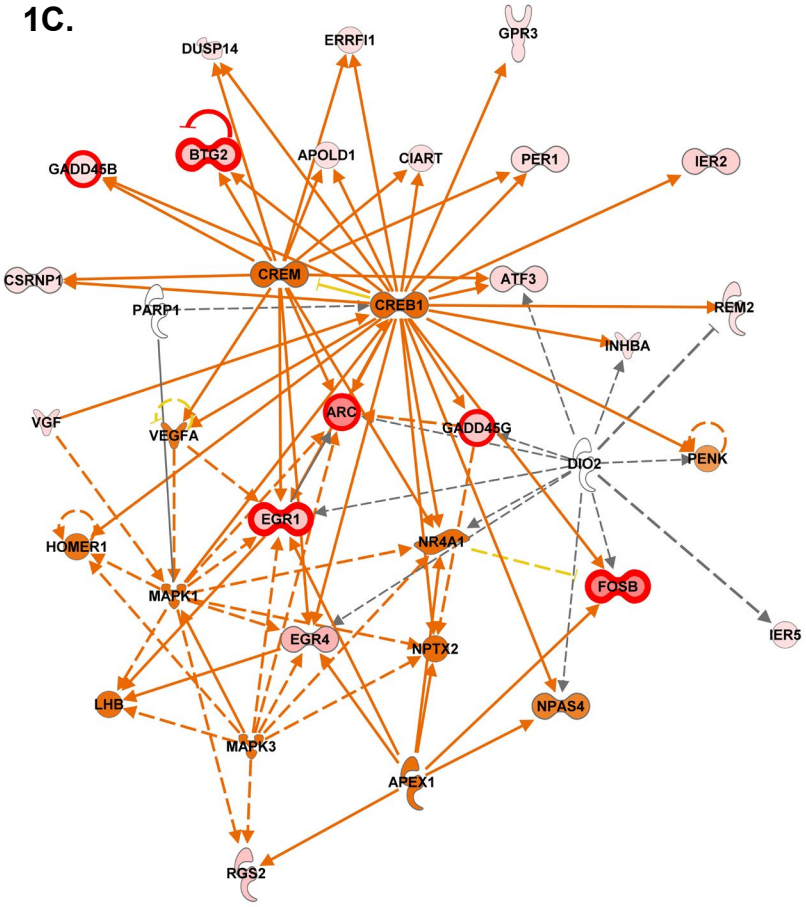

2A.

	p-value	Activation Score
Cell death of hippocampal neurons	8.02E-05	-2.410
Apoptosis	4.95E-07	-2.003
Neuronal cell death	1.68E-05	-1.974
Cell death of cerebral cortex cells	0.000146	-1.589
Degeneration of neurons	0.0309	-0.660
Cell death of neuroglia	0.00234	-0.339
Cell death of cortical neurons	0.033	-0.283
Apoptosis of granule cells	6.06E-05	-0.266
Apoptosis of neuroglia	0.00413	-0.152
Apoptosis of sympathetic neuron	0.000254	-0.145
Cell viability of hippocampal neurons	0.00023	1.124
Cell viability of cerebral cortex cells	0.000519	1.413
Survival of cephalic neurons	0.000519	1.413
Survival of neural cells	0.0241	1.774
Cell viability	0.0263	1.774

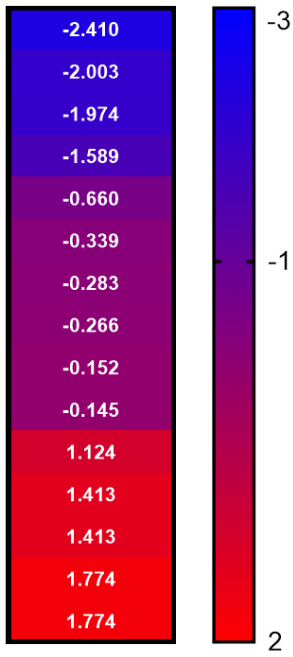

2B.

	p-value	Activation Score
Proliferation of neuroglia	0.00193	-0.314
Formation of dendritic spines	0.0147	0.577
Formation of dendrites	0.0284	0.577
Growth of dendrites	0.00487	1.082
Dendritic growth/branching	0.000413	1.090
Density of dendritic spines	0.02	1.165
Axonogenesis	0.0156	1.412
Branching of neurons	5.32E-05	1.587
Proliferation of neural cells	0.00537	1.627
Neuritogenesis	5.03E-06	1.913
Branching of axons	0.00933	1.922
Branching of neurites	0.000164	1.924
Outgrowth of neurites	0.0169	1.988
Growth of neurites	0.0122	2.238
Development of neurons	1.27E-06	2.286

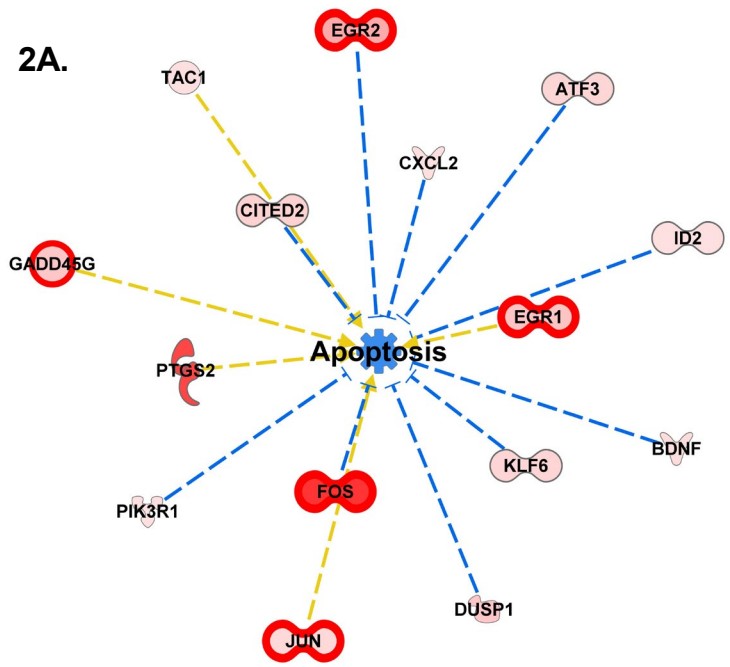

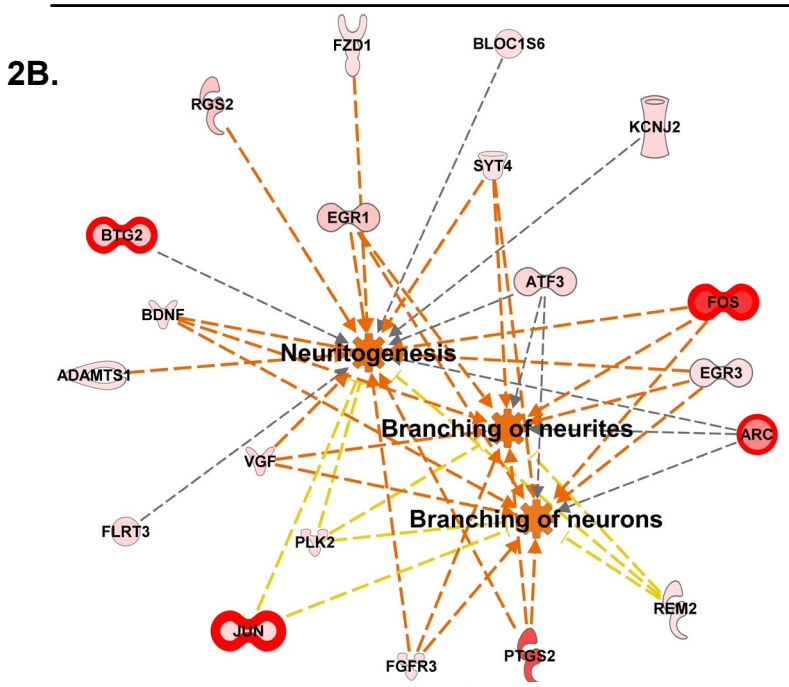

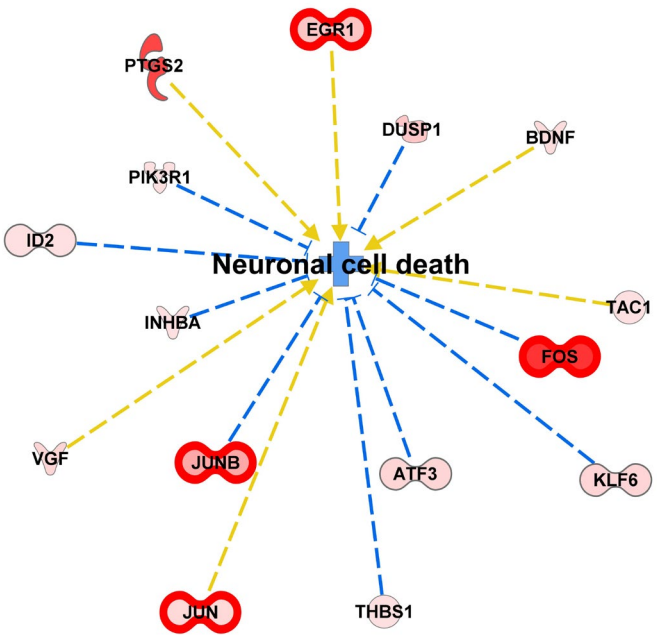

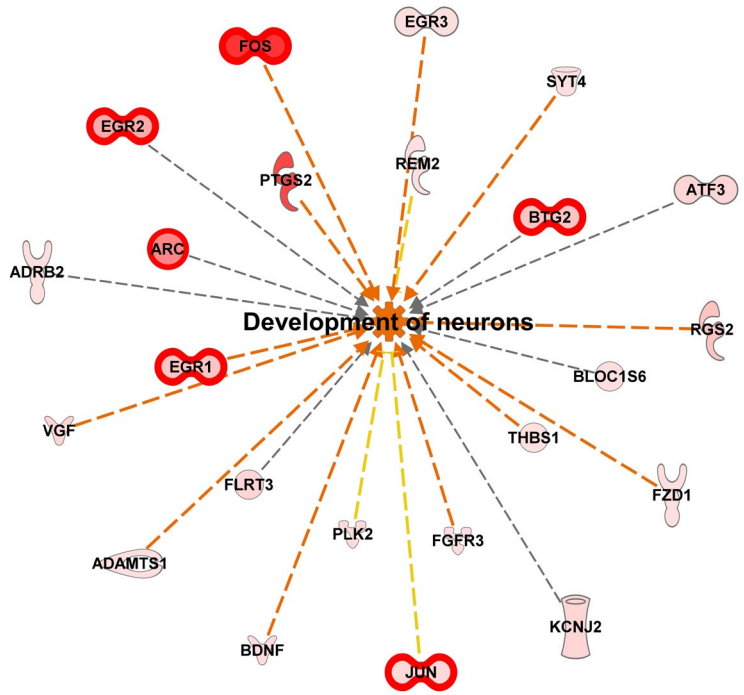

3A.

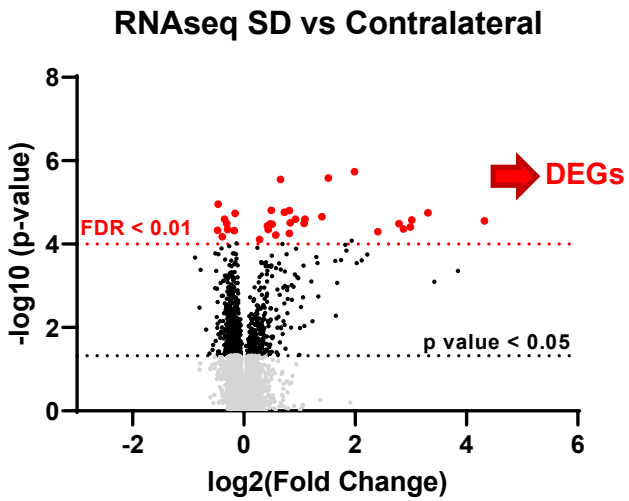

	log2 FC	Adj.Pval
NPAS4	7.13	3.48E-41
FOS	4.44	7.69E-62
PTGS2	4.29	2.10E-22
FOSB	3.61	7.13E-20
DUSP6	3.12	1.85E-38
ARC	3.06	1.34E-47
NR4A1	2.95	3.61E-39
JUNB	2.86	6.60E-44
EGR2	2.73	1.21E-04
EGR4	2.49	1.58E-20
DUSP5	2.41	1.04E-07
RGS2	2.13	1.36E-15
BTG2	2.09	2.89E-10
TRIB1	2.07	2.12E-02
EGR1	1.98	4.75E-22
DUSP1	1.92	2.96E-13
ARL4D	1.89	4.35E-21
IER2	1.88	4.67E-06
GADD45G	1.81	1.88E-17
NPTX2	1.76	9.55E-07
ADRB1	1.72	9.83E-05

Fold Change

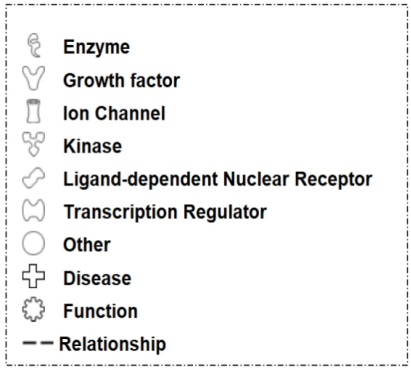

3B.

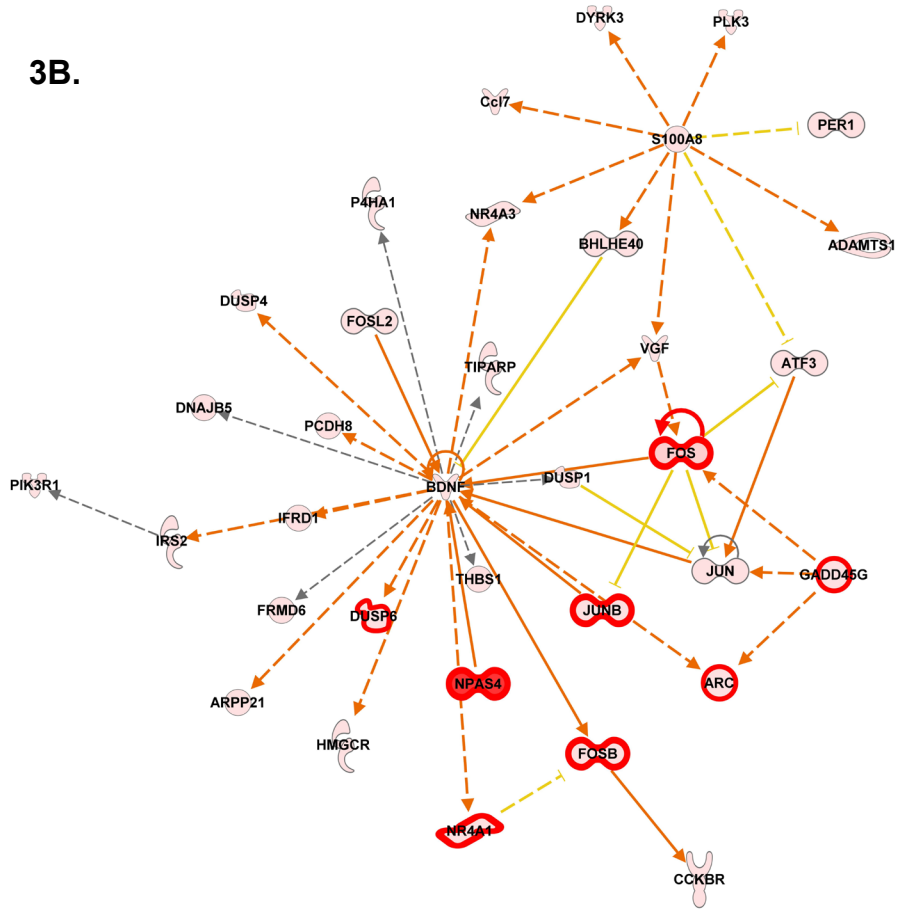

3C.

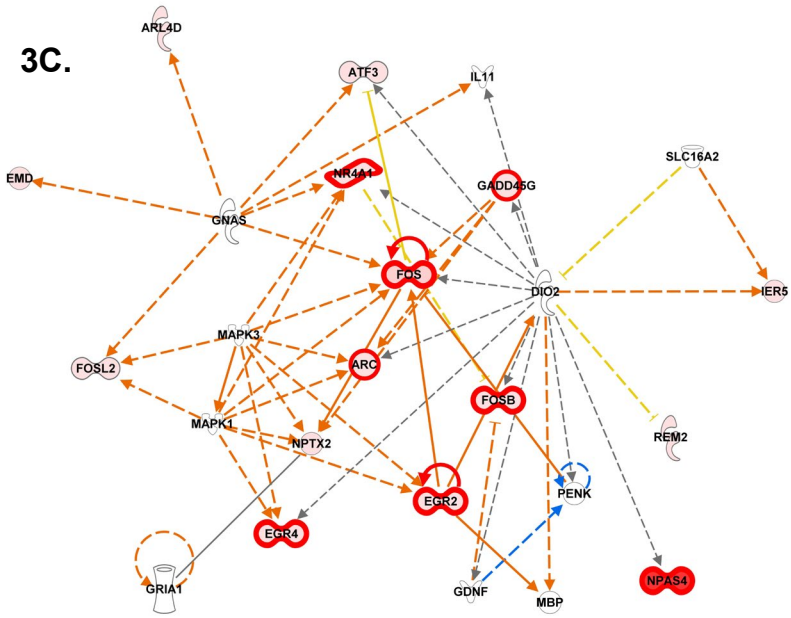

4A.

	p-value	Activation Score
Cell death of hippocampal neurons	0.0015	-1.958
Apoptosis	9.12E-08	-1.197
Neuronal cell death	8.64E-06	-0.903
Cell death of cerebral cortex cells	0.00133	-0.838
Apoptosis of neuroglia	0.00107	-0.152
Apoptosis of sympathetic neuron	6.08E-05	-0.145
Apoptosis of granule cells	0.000199	0.063
Cell death of cortical neurons	0.0346	0.173
Cell viability of cerebral cortex cells	0.00112	1.126
Survival of cephalic neurons	0.00112	1.126
Survival of neural cells	0.0188	1.475
Cell viability	0.0203	1.475

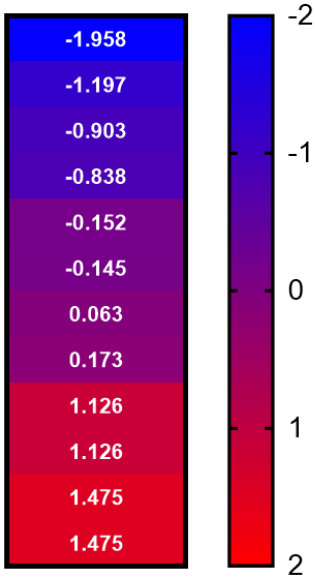

4B.

	p-value	Activation Score
Proliferation of neuroglia	0.00204	0.784
Differentiation of neuroglia	0.00708	1.090
Dendritic growth/branching	0.000278	1.412
Axonogenesis	0.00923	1.587
Branching of neurons	0.000015	1.772
Outgrowth of neurites	0.0255	1.912
Development of neural cells	7.62E-07	1.922
Branching of axons	0.00252	1.924
Branching of neurites	6.03E-05	1.985
Growth of dendrites	0.00127	2.048
Neuritogenesis	4.43E-06	2.183
Differentiation of neural cells	0.000945	2.224
Development of neurons	1.3E-06	

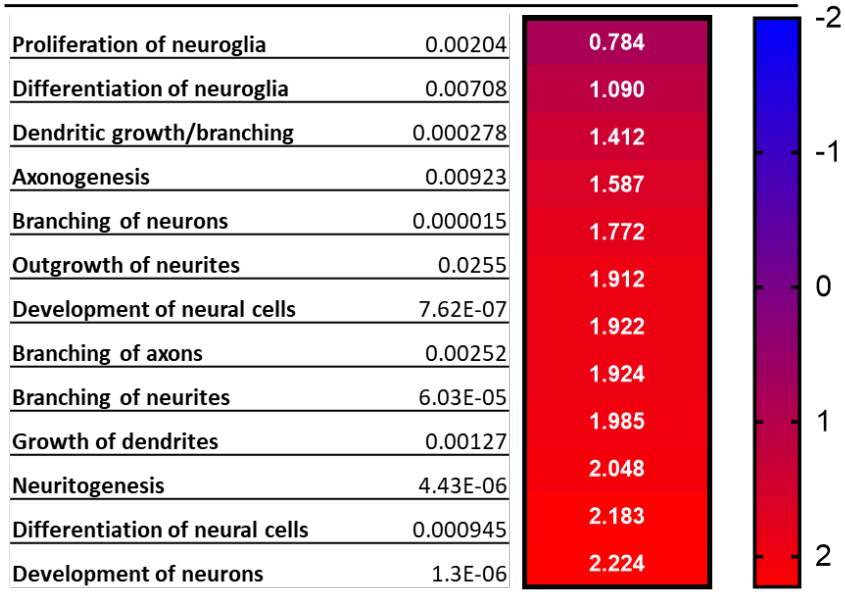

4A.

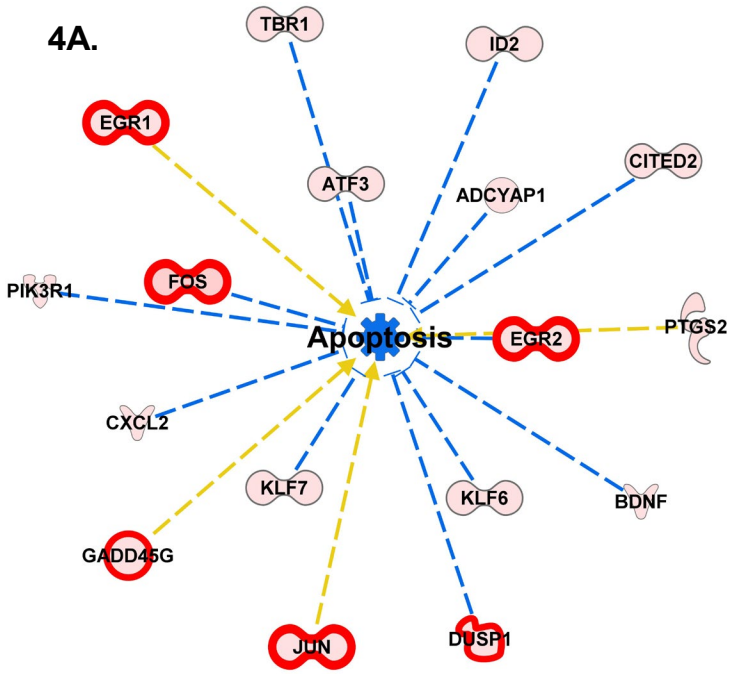

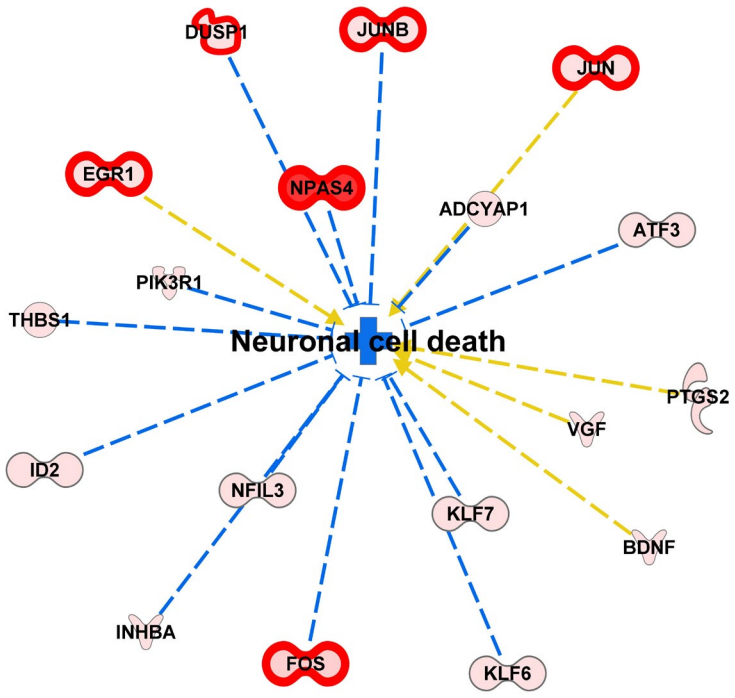

4B.

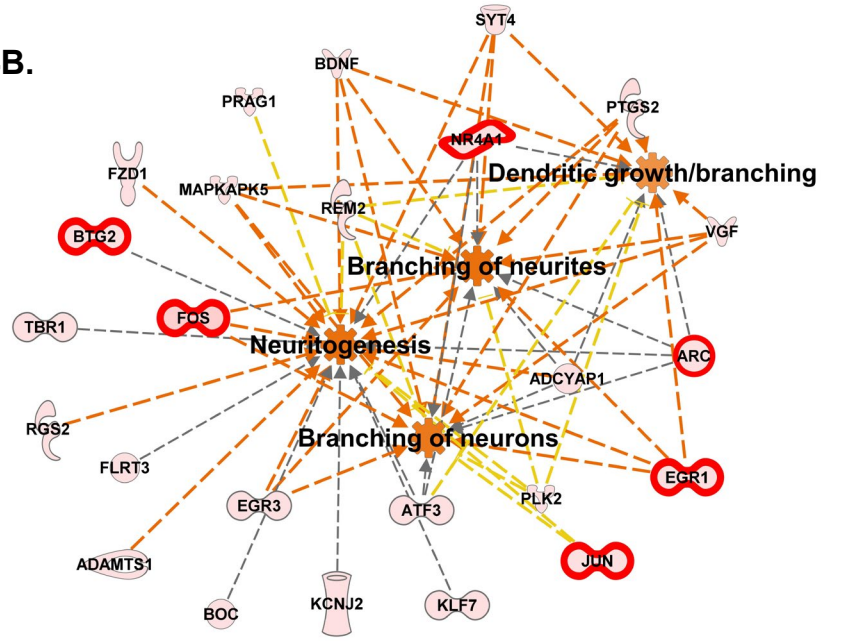

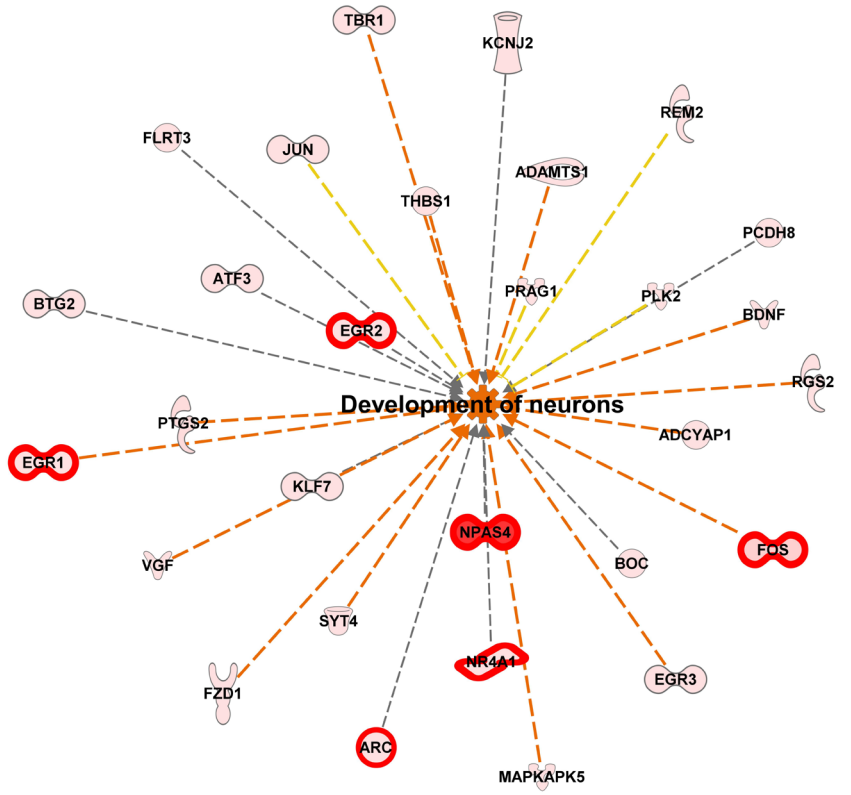

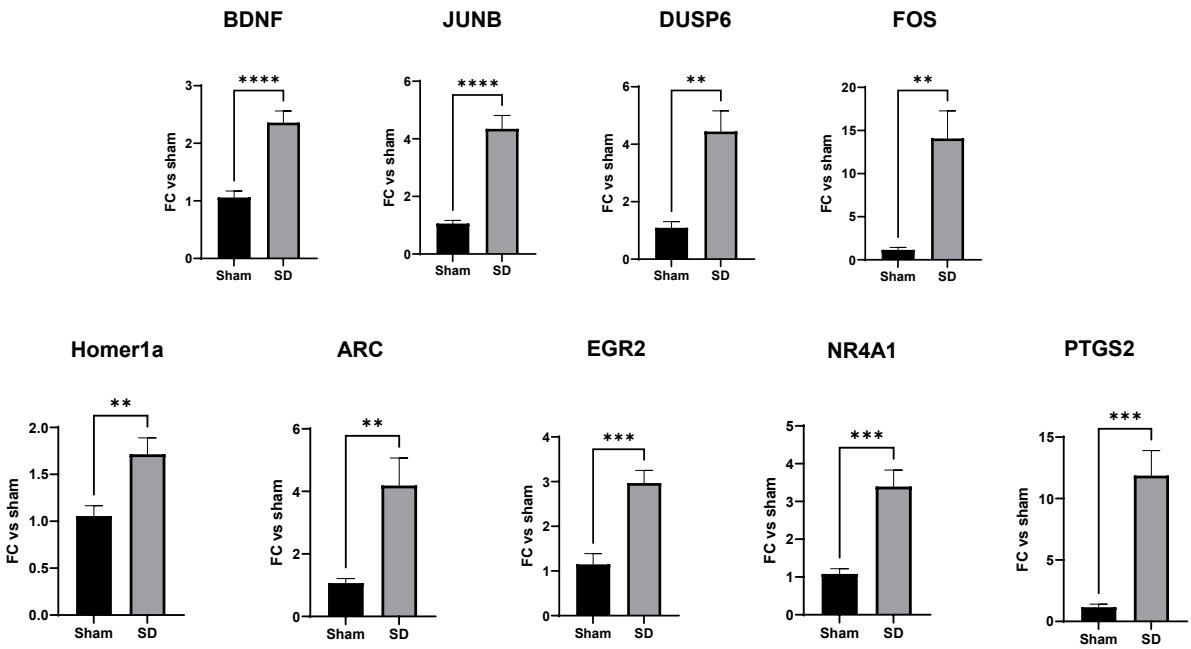
BDNF
JUNB
DUSP6
FOS
Homer1a
ARC
EGR2
NR4A1
PTGS2
FC vs sham
Sham
SD
****
**
***

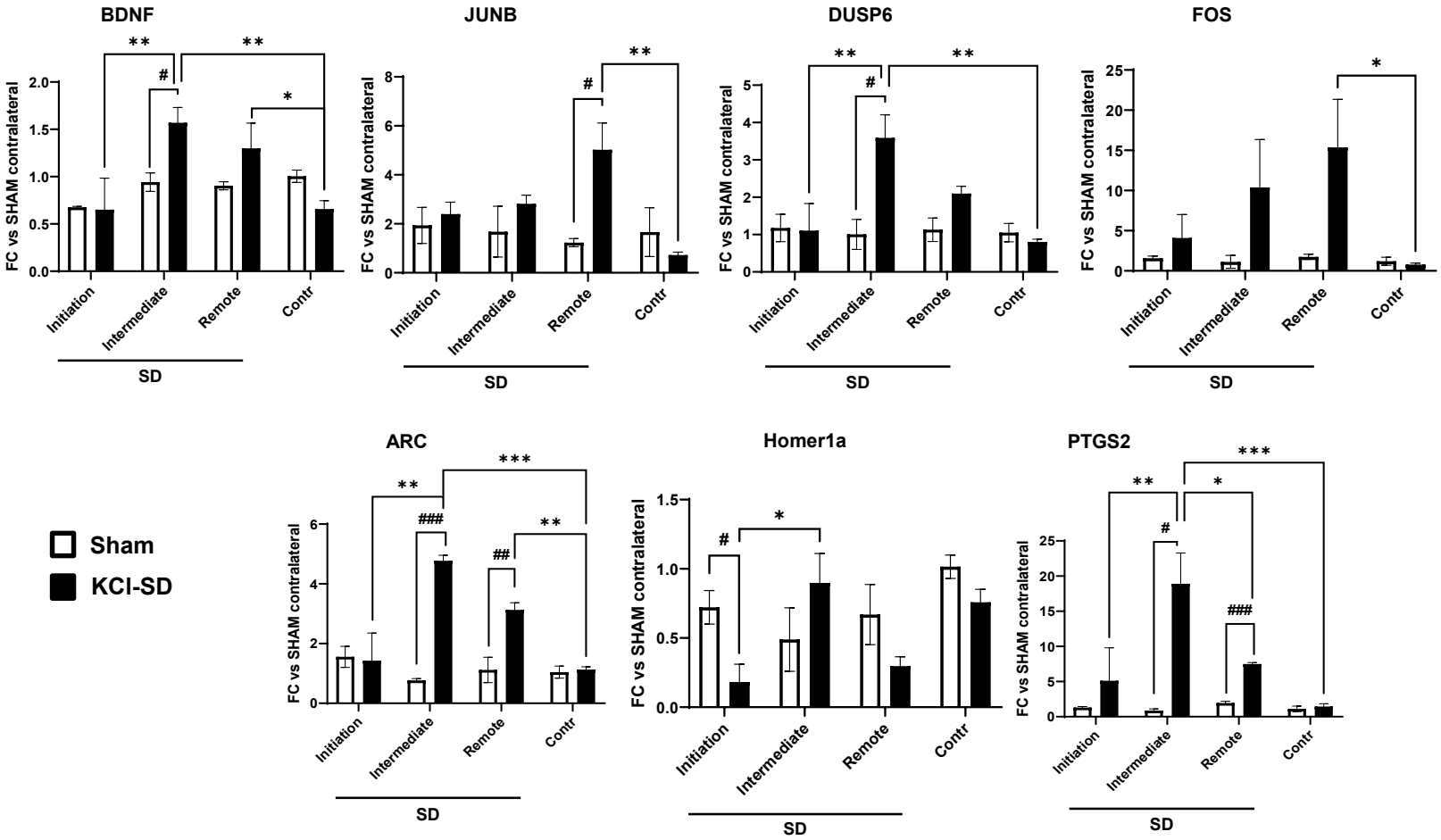
BDNF
JUNB
DUSP6
FOS
ARC
Homer1a
PTGS2
FC vs SHAM contralateral
Initiation
Intermediate
Remote
Contr
SD
Sham
KCI-SD

Sup Figure 1

1A.

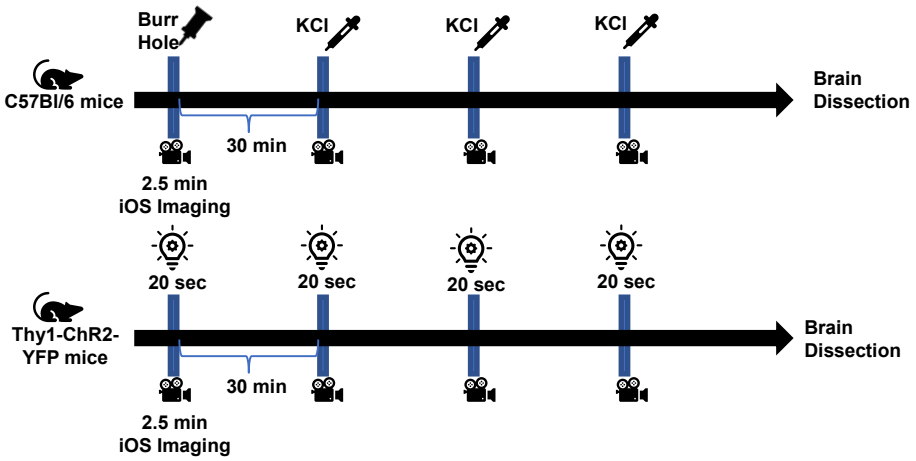

1B.

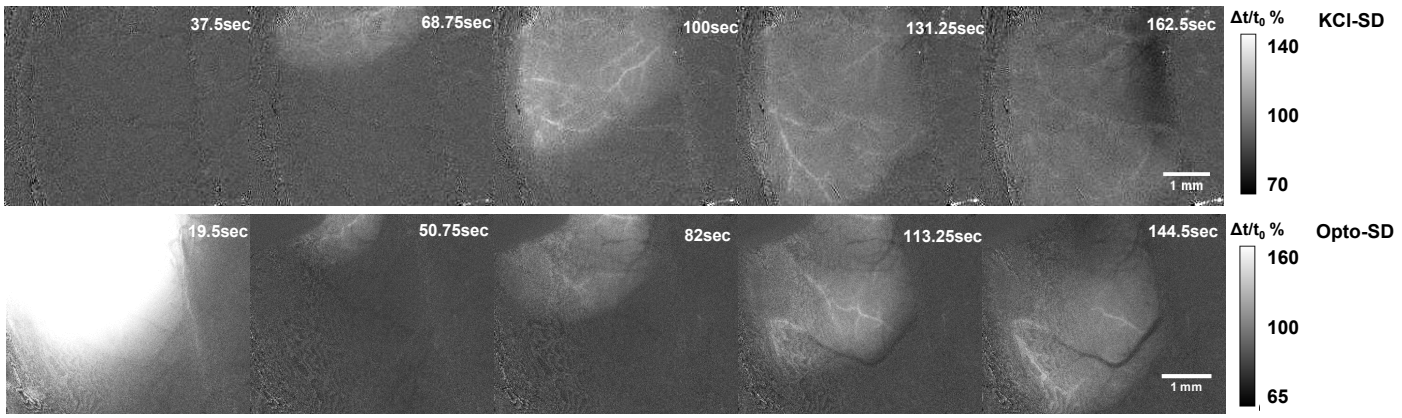

Sup Figure 2

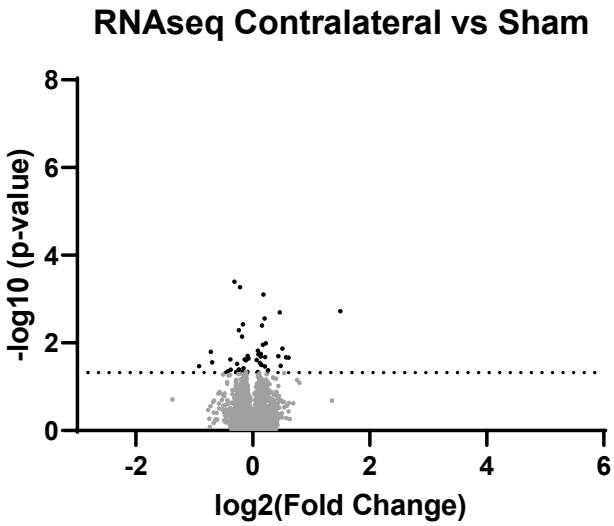
RNAseq Contralateral vs Sham
-log10 (p-value)
8
6
4
2
0
-2
0
2
4
6
log2(Fold Change)

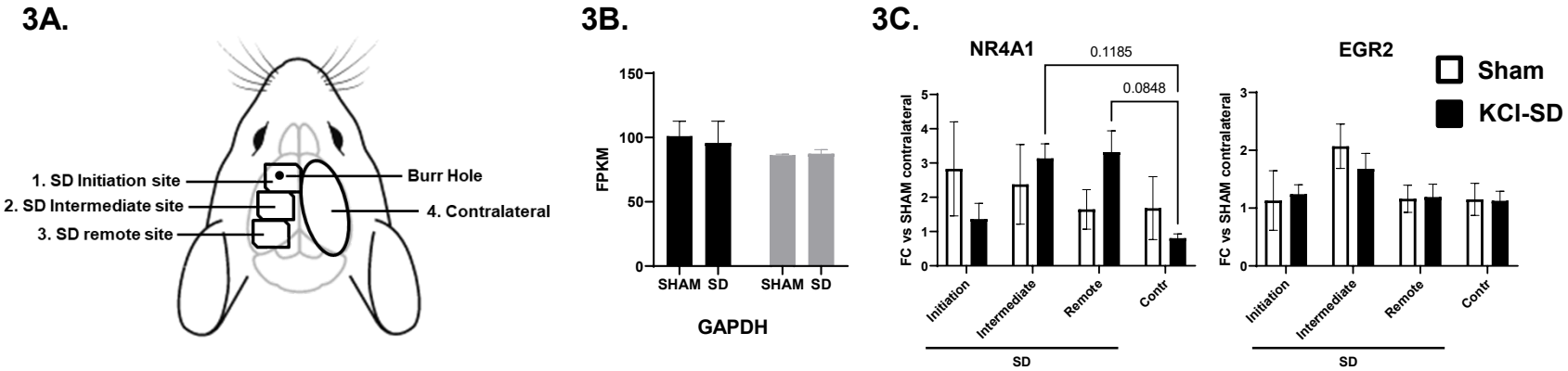
3A.
1. SD Initiation site
2. SD Intermediate site
3. SD remote site
Burr Hole
4. Contralateral
3B.
FPKM
150
100
50
0
SHAM SD SHAM SD
GAPDH
3C.
NR4A1
0.1185
0.0848
FC vs SHAM contralateral
Initiation
Intermediate
Remote
Contr
SD
EGR2
Sham
KCl-SD

1A.

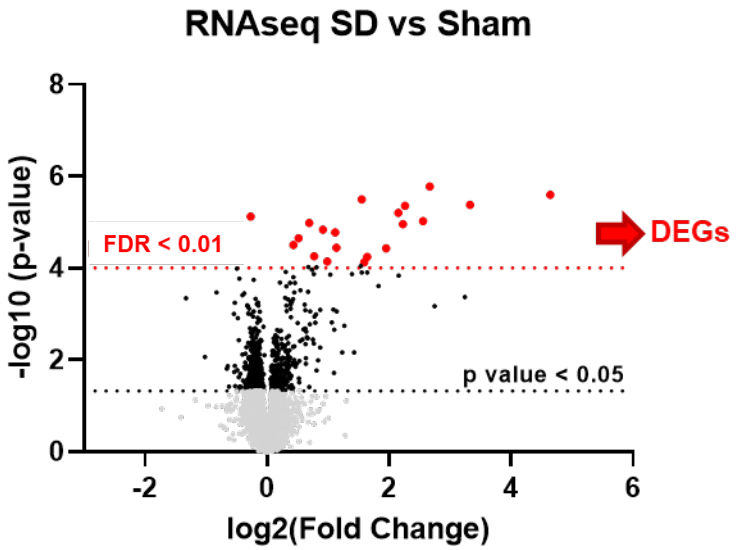

	log2 FC	Adj.Pval
NPAT	4.58	7.44E-04
PTGS2	3.32	1.38E-15
FOS	3.10	1.61E-12
EGR2	2.73	1.63E-04
FOSB	2.61	1.61E-12
ARC	2.50	6.13E-19
DUSP6	2.14	2.26E-08
JUNB	2.12	3.32E-15
DUSP5	2.05	3.45E-06
EGR4	1.97	4.92E-13
ARL4D	1.67	3.95E-15
RGS2	1.63	2.01E-06
GADD45G	1.58	3.22E-10
BTG2	1.57	1.90E-04
DUSP1	1.55	2.81E-07
EGR1	1.52	3.02E-12

Fold Change

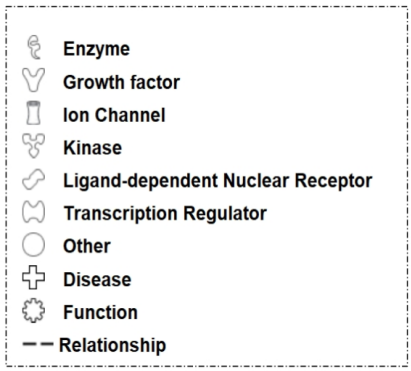

1B.

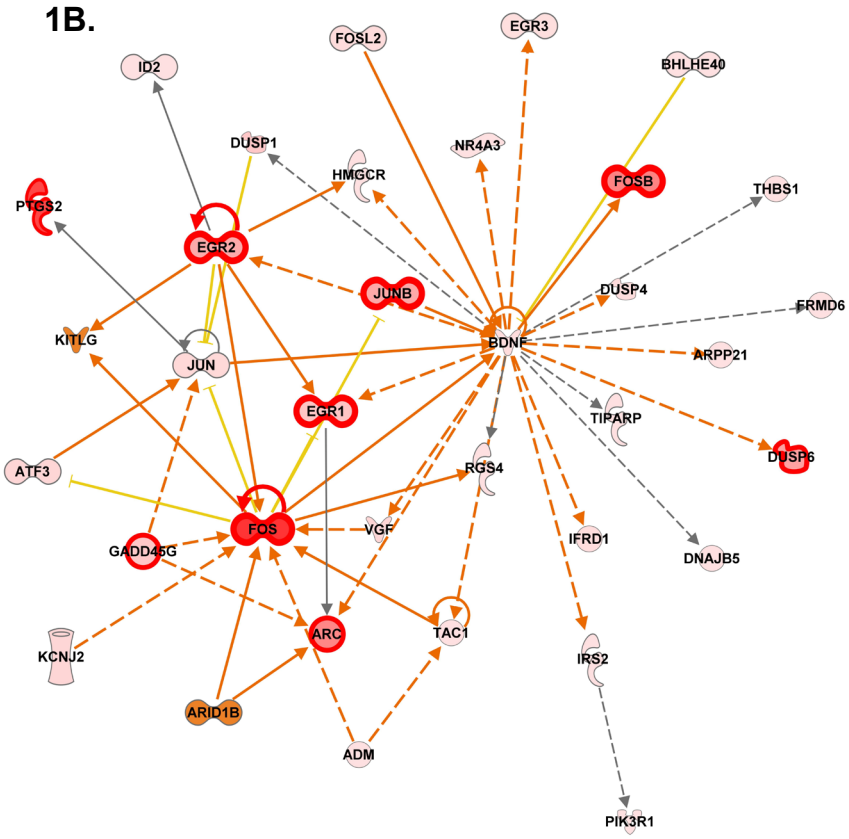

1C.

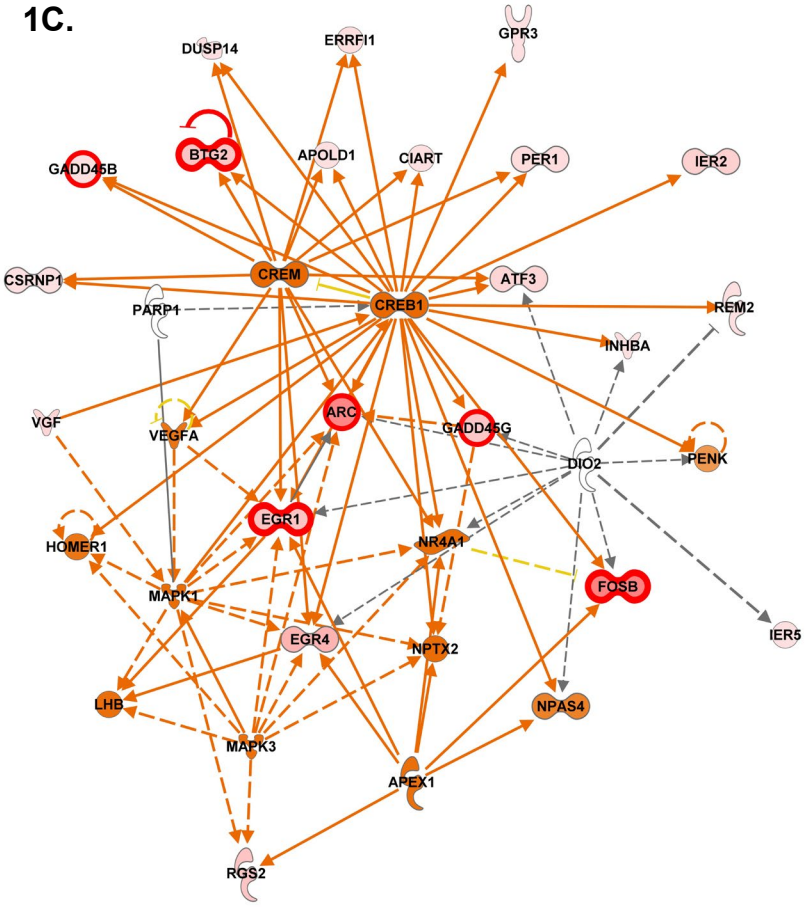

2A.

	p-value	Activation Score
Cell death of hippocampal neurons	8.02E-05	-2.410
Apoptosis	4.95E-07	-2.003
Neuronal cell death	1.68E-05	-1.974
Cell death of cerebral cortex cells	0.000146	-1.589
Degeneration of neurons	0.0309	-0.660
Cell death of neuroglia	0.00234	-0.339
Cell death of cortical neurons	0.033	-0.283
Apoptosis of granule cells	6.06E-05	-0.266
Apoptosis of neuroglia	0.00413	-0.152
Apoptosis of sympathetic neuron	0.000254	-0.145
Cell viability of hippocampal neurons	0.00023	1.124
Cell viability of cerebral cortex cells	0.000519	1.413
Survival of cephalic neurons	0.000519	1.413
Survival of neural cells	0.0241	1.774
Cell viability	0.0263	1.774

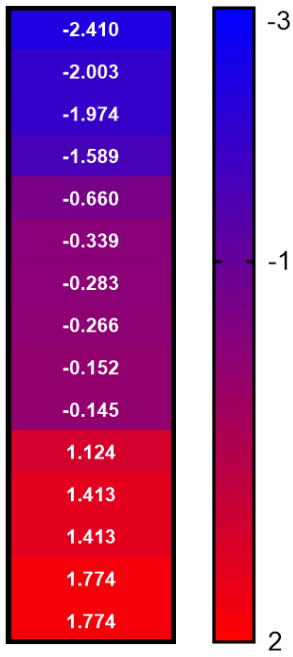

2B.

	p-value	Activation Score
Proliferation of neuroglia	0.00193	-0.314
Formation of dendritic spines	0.0147	0.577
Formation of dendrites	0.0284	0.577
Growth of dendrites	0.00487	1.082
Dendritic growth/branching	0.000413	1.090
Density of dendritic spines	0.02	1.165
Axonogenesis	0.0156	1.412
Branching of neurons	5.32E-05	1.587
Proliferation of neural cells	0.00537	1.627
Neuritogenesis	5.03E-06	1.913
Branching of axons	0.00933	1.922
Branching of neurites	0.000164	1.924
Outgrowth of neurites	0.0169	1.988
Growth of neurites	0.0122	2.238
Development of neurons	1.27E-06	2.286

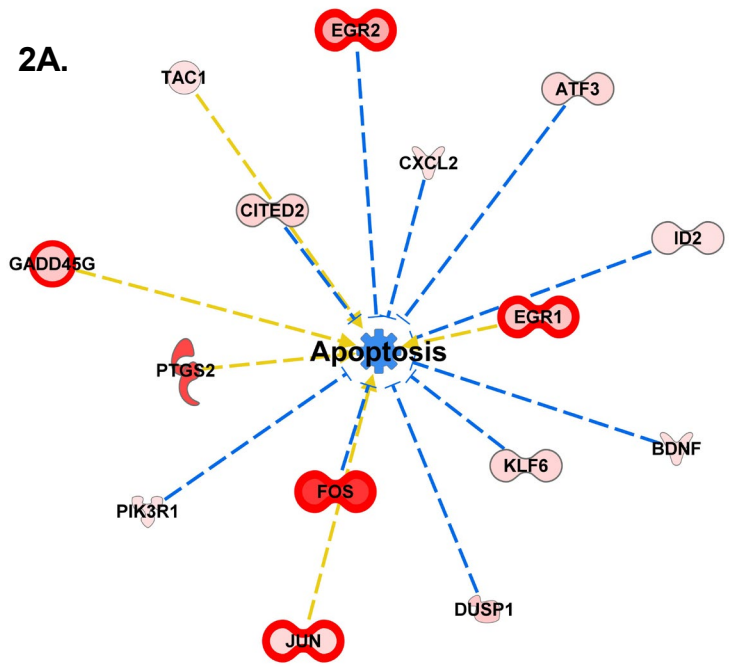

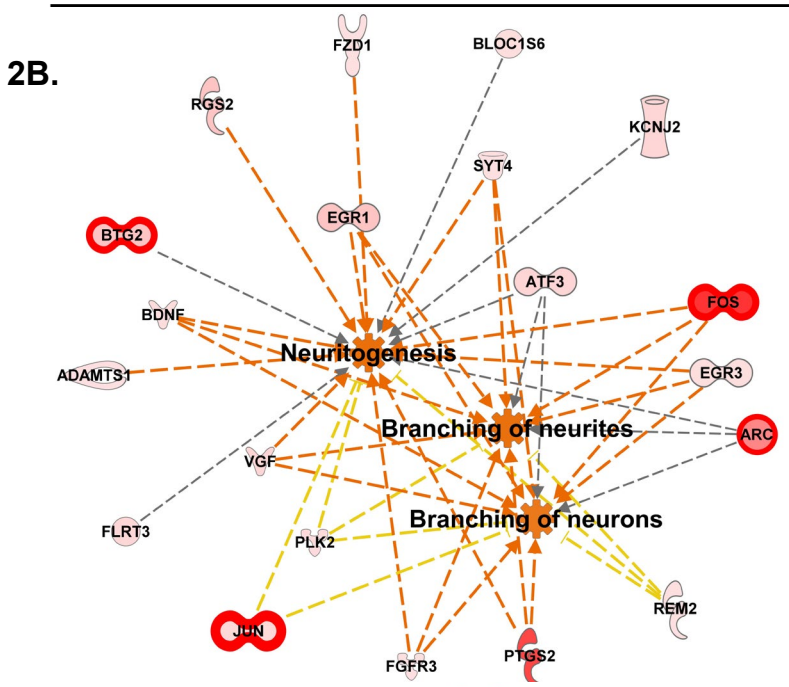

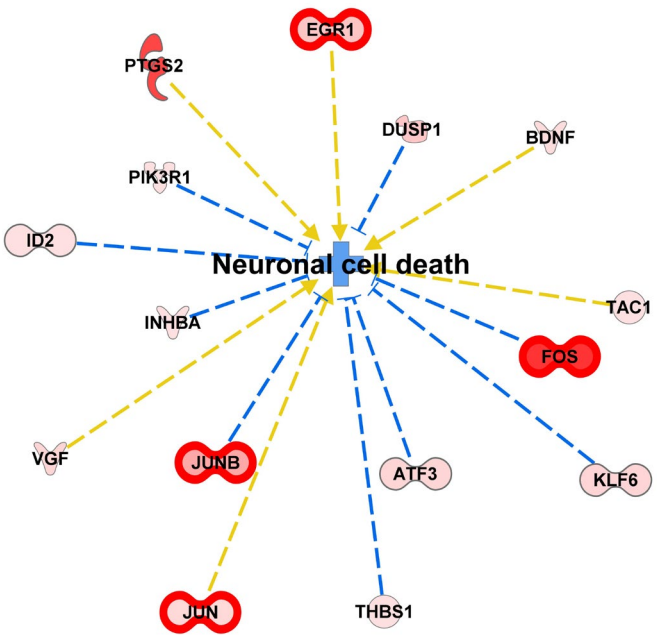

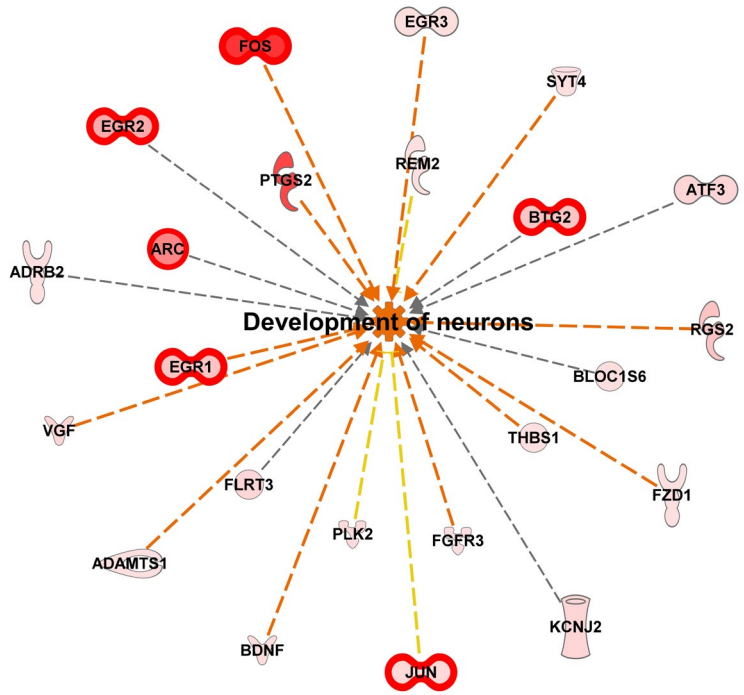

3A.

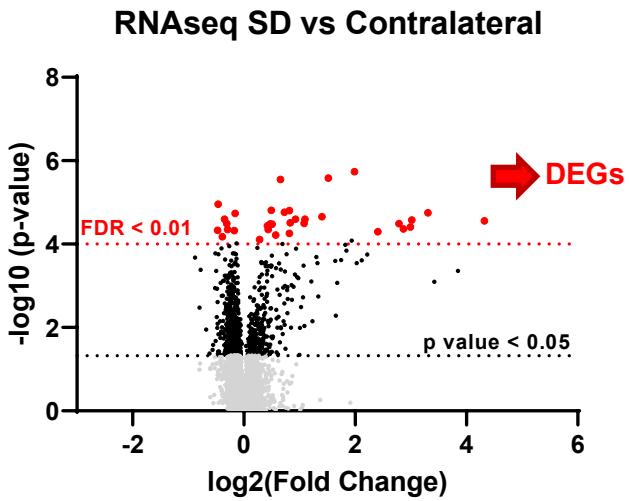

	log2 FC	Adj.Pval
NPAS4	7.13	3.48E-41
FOS	4.44	7.69E-62
PTGS2	4.29	2.10E-22
FOSB	3.61	7.13E-20
DUSP6	3.12	1.85E-38
ARC	3.06	1.34E-47
NR4A1	2.95	3.61E-39
JUNB	2.86	6.60E-44
EGR2	2.73	1.21E-04
EGR4	2.49	1.58E-20
DUSP5	2.41	1.04E-07
RGS2	2.13	1.36E-15
BTG2	2.09	2.89E-10
TRIB1	2.07	2.12E-02
EGR1	1.98	4.75E-22
DUSP1	1.92	2.96E-13
ARL4D	1.89	4.35E-21
IER2	1.88	4.67E-06
GADD45G	1.81	1.88E-17
NPTX2	1.76	9.55E-07
ADRB1	1.72	9.83E-05

Fold Change

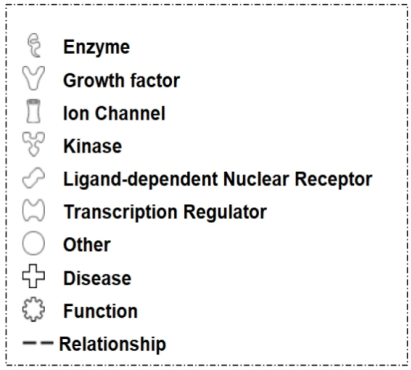

3B.

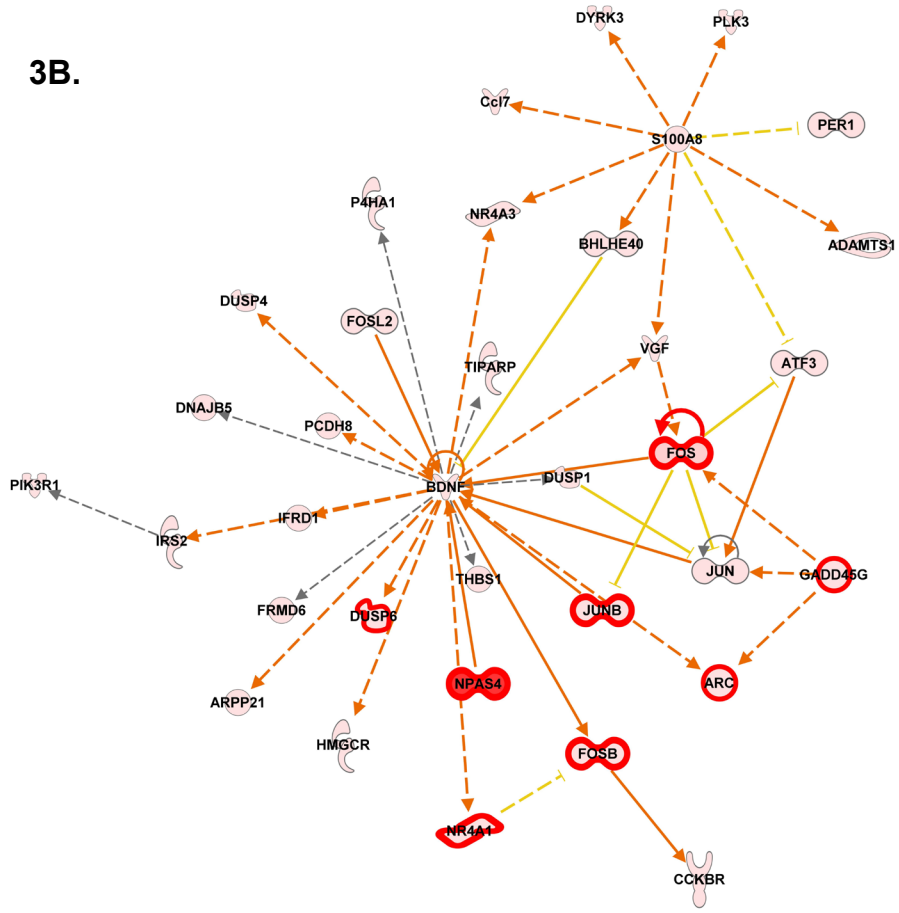

3C.

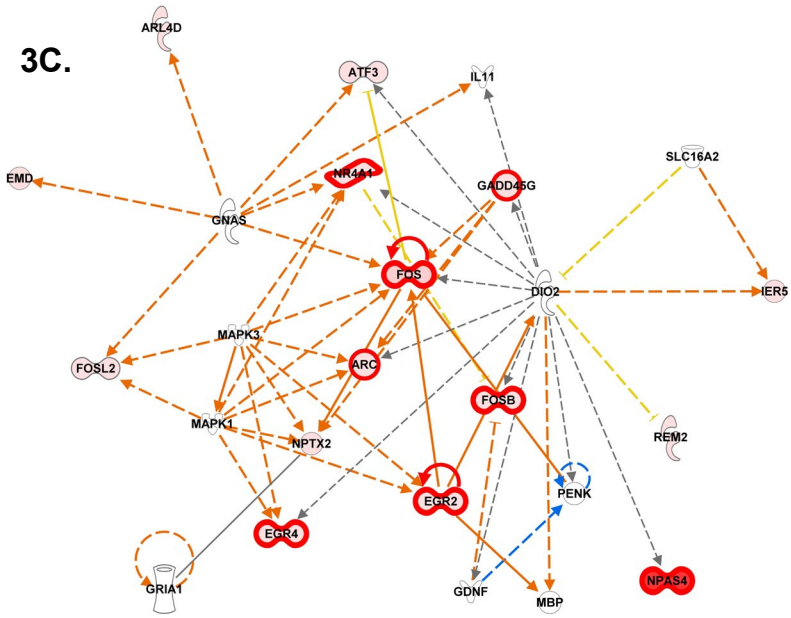

4A.

	p-value	Activation Score
Cell death of hippocampal neurons	0.0015	-1.958
Apoptosis	9.12E-08	-1.197
Neuronal cell death	8.64E-06	-0.903
Cell death of cerebral cortex cells	0.00133	-0.838
Apoptosis of neuroglia	0.00107	-0.152
Apoptosis of sympathetic neuron	6.08E-05	-0.145
Apoptosis of granule cells	0.000199	0.063
Cell death of cortical neurons	0.0346	0.173
Cell viability of cerebral cortex cells	0.00112	1.126
Survival of cephalic neurons	0.00112	1.126
Survival of neural cells	0.0188	1.475
Cell viability	0.0203	1.475

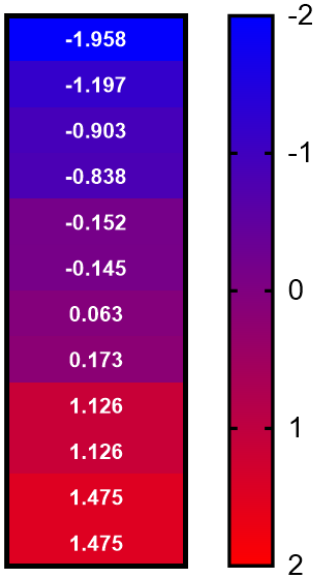

4B.

	p-value	Activation Score
Proliferation of neuroglia	0.00204	0.784
Differentiation of neuroglia	0.00708	1.090
Dendritic growth/branching	0.000278	1.412
Axonogenesis	0.00923	1.587
Branching of neurons	0.000015	1.772
Outgrowth of neurites	0.0255	1.912
Development of neural cells	7.62E-07	1.922
Branching of axons	0.00252	1.924
Branching of neurites	6.03E-05	1.985
Growth of dendrites	0.00127	2.048
Neuritogenesis	4.43E-06	2.183
Differentiation of neural cells	0.000945	2.224
Development of neurons	1.3E-06	

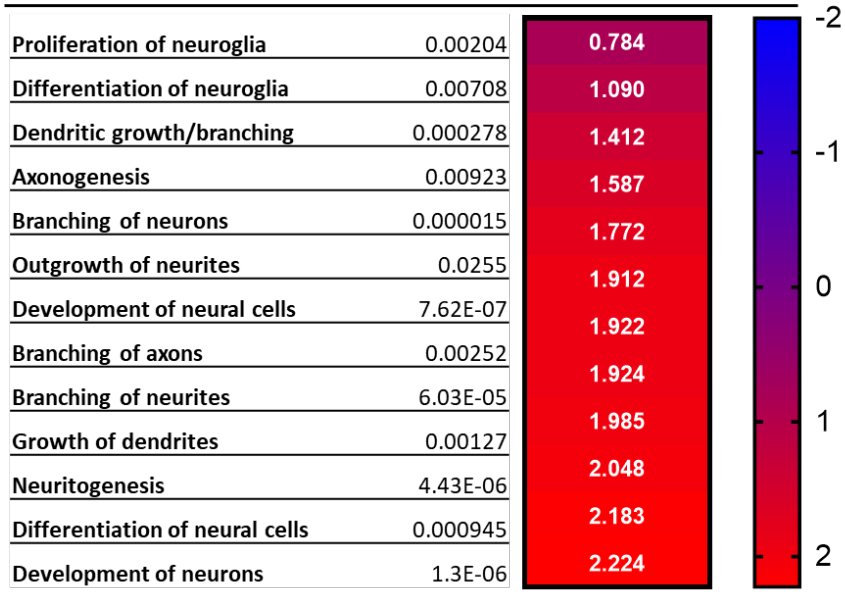

4A.

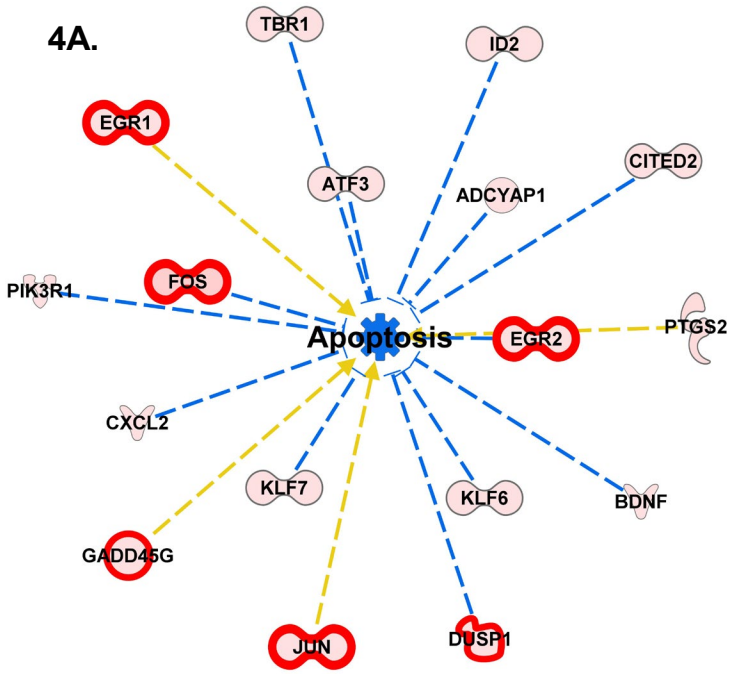

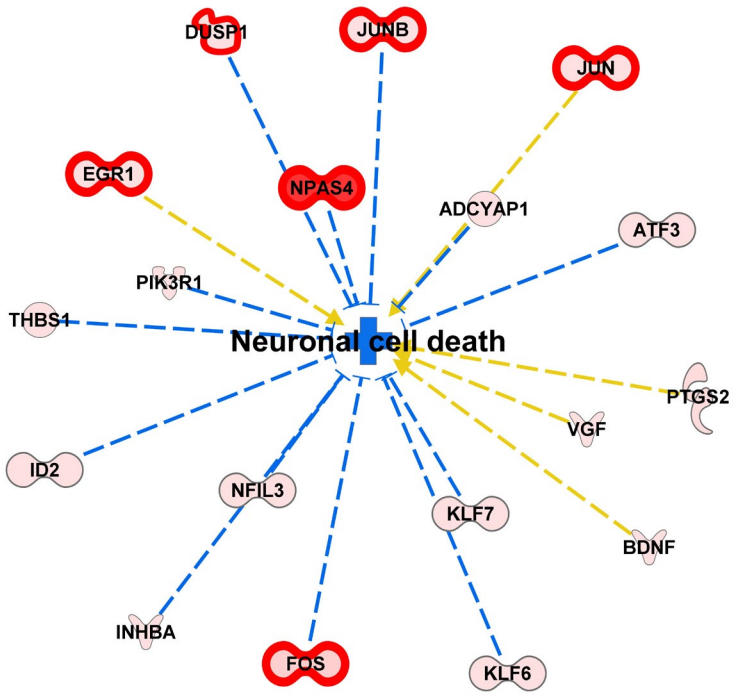

4B.

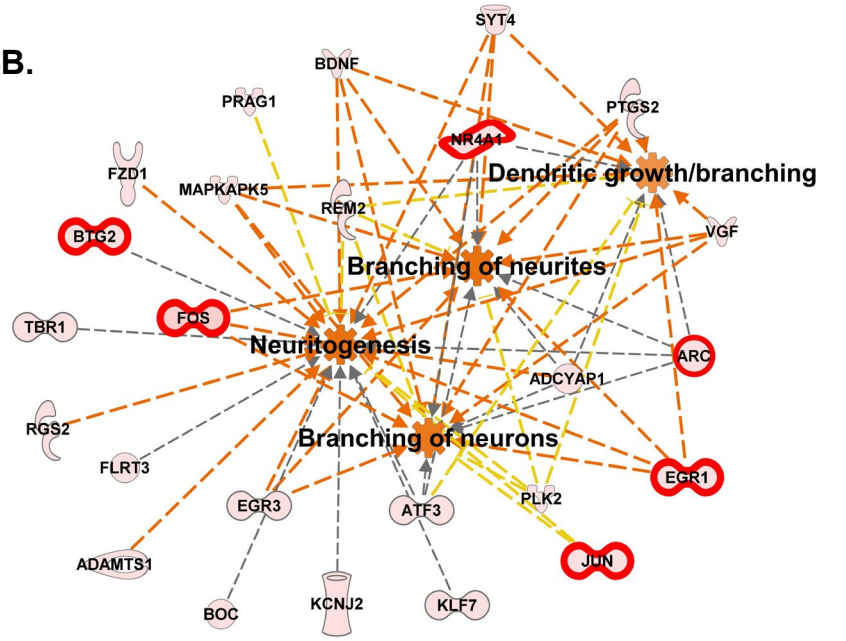

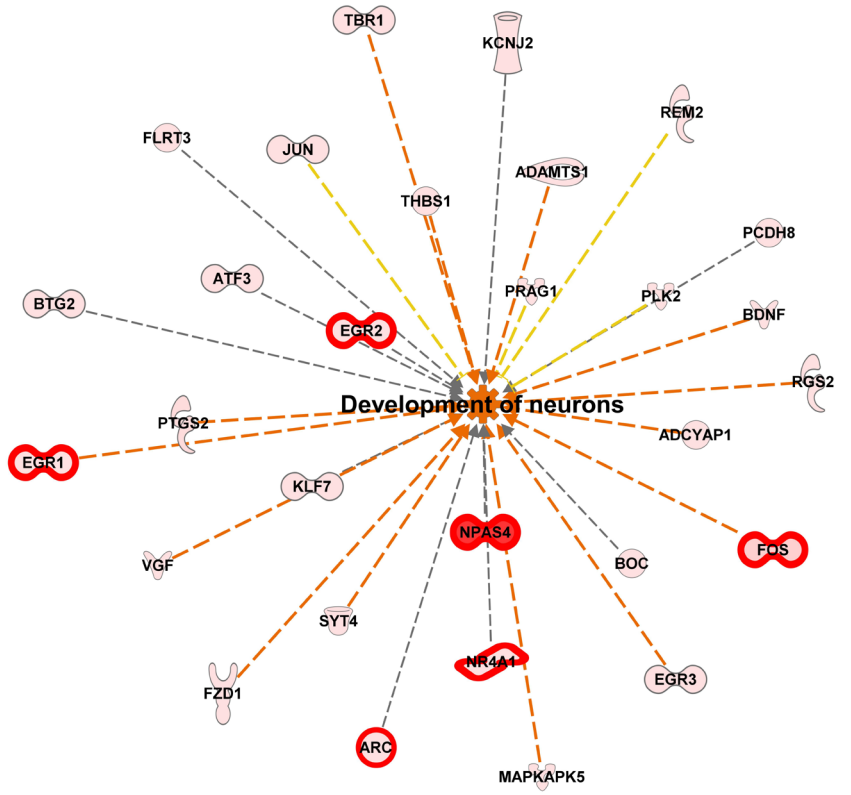

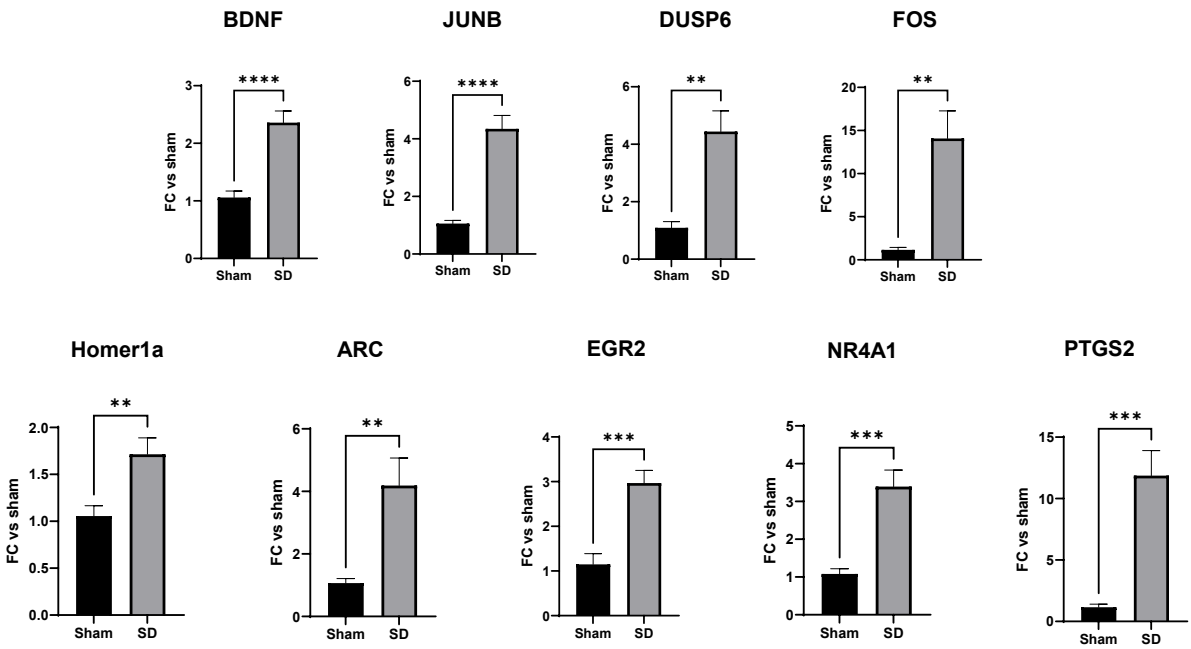
BDNF
JUNB
DUSP6
FOS
Homer1a
ARC
EGR2
NR4A1
PTGS2
FC vs sham
Sham
SD
****
**
***

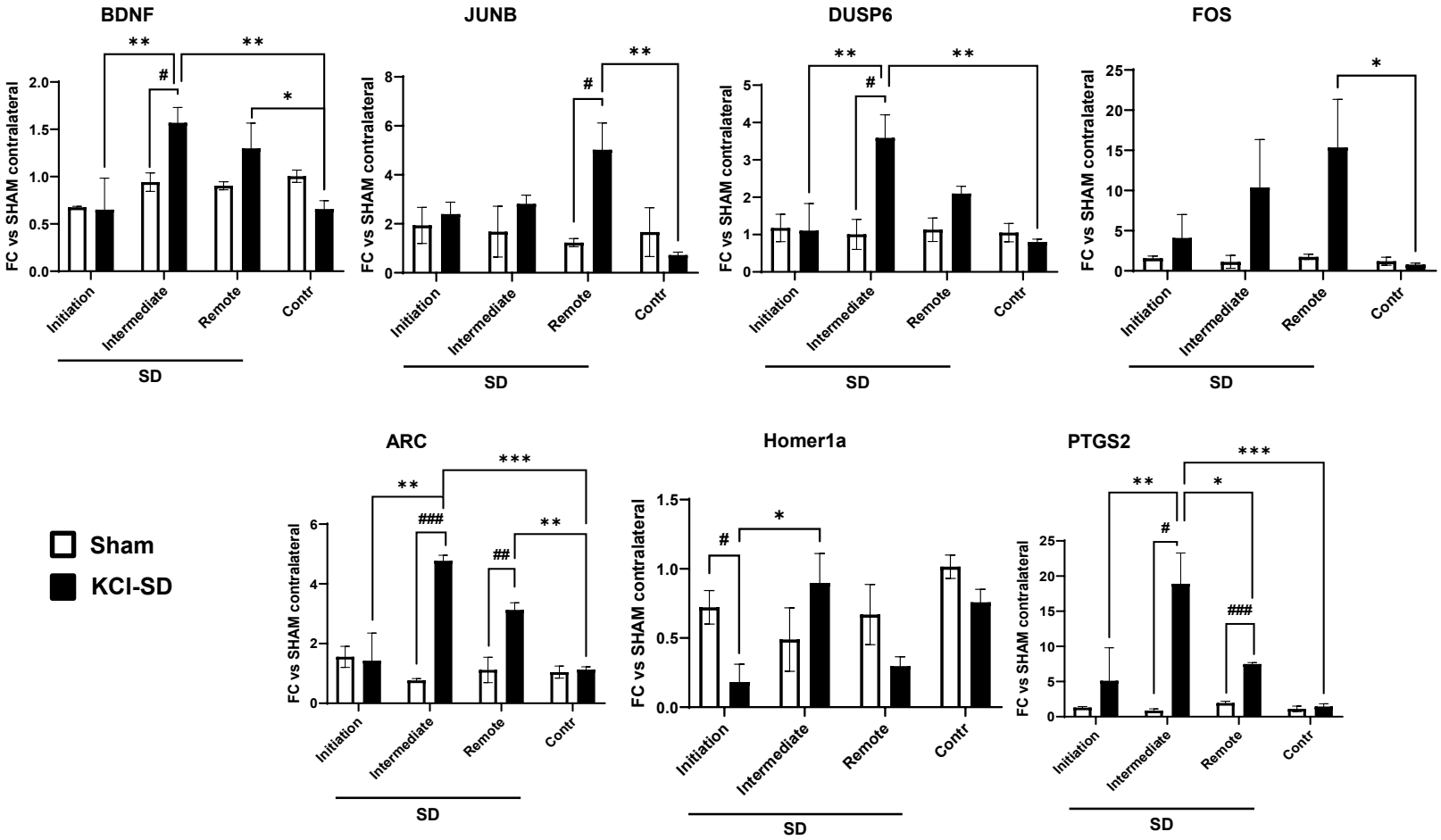
BDNF
JUNB
DUSP6
FOS
ARC
Homer1a
PTGS2
FC vs SHAM contralateral
Initiation
Intermediate
Remote
Contr
SD
Sham
KCI-SD

Sup Figure 1

1A.

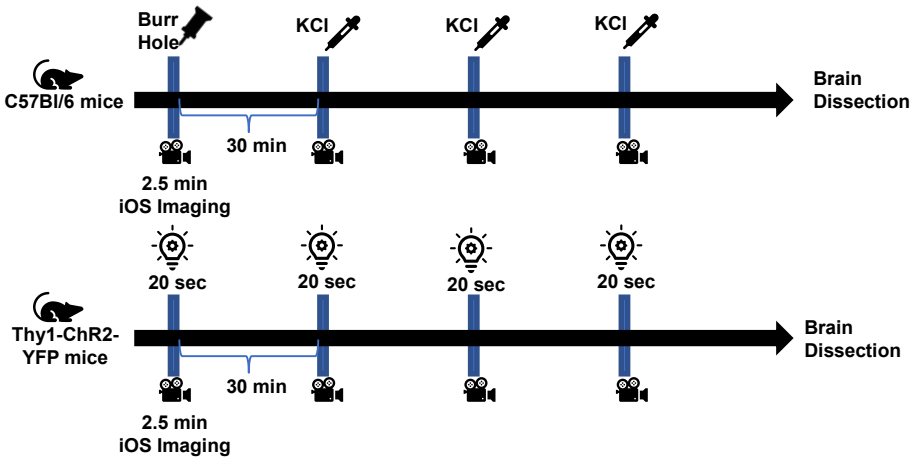

1B.

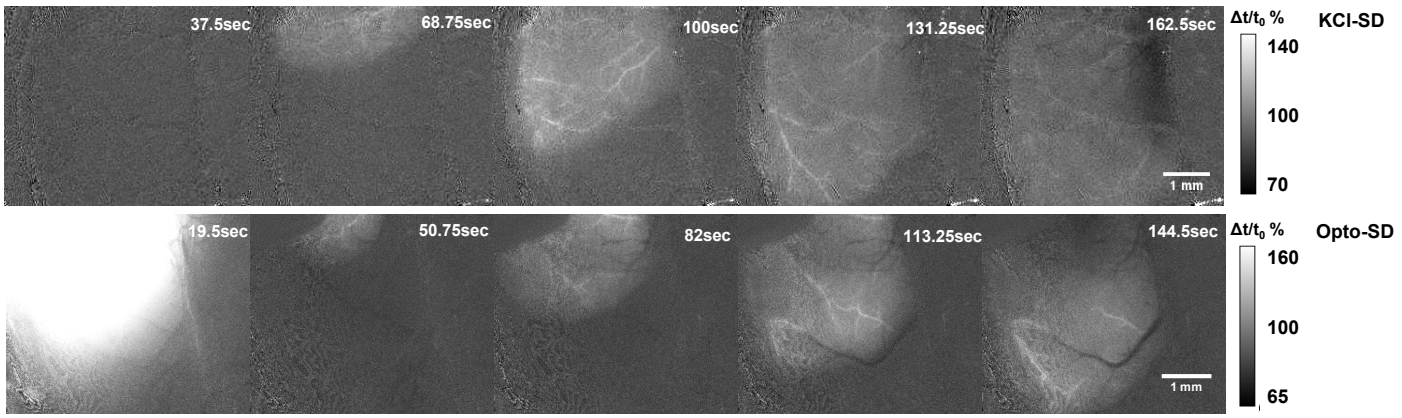

Sup Figure 2

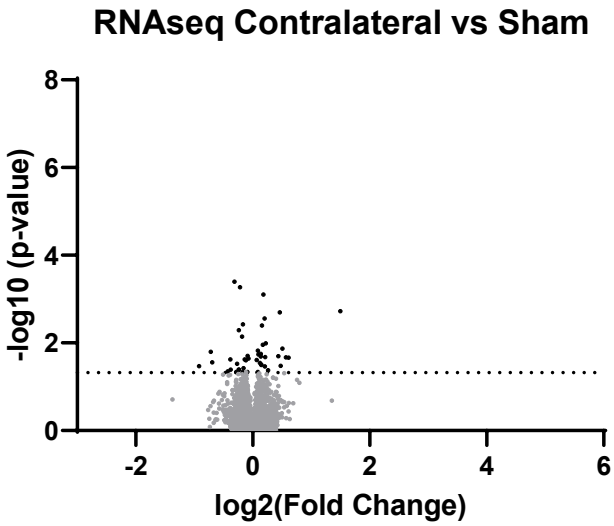
RNAseq Contralateral vs Sham
-log10 (p-value)
8
6
4
2
0
-2
0
2
4
6
log2(Fold Change)

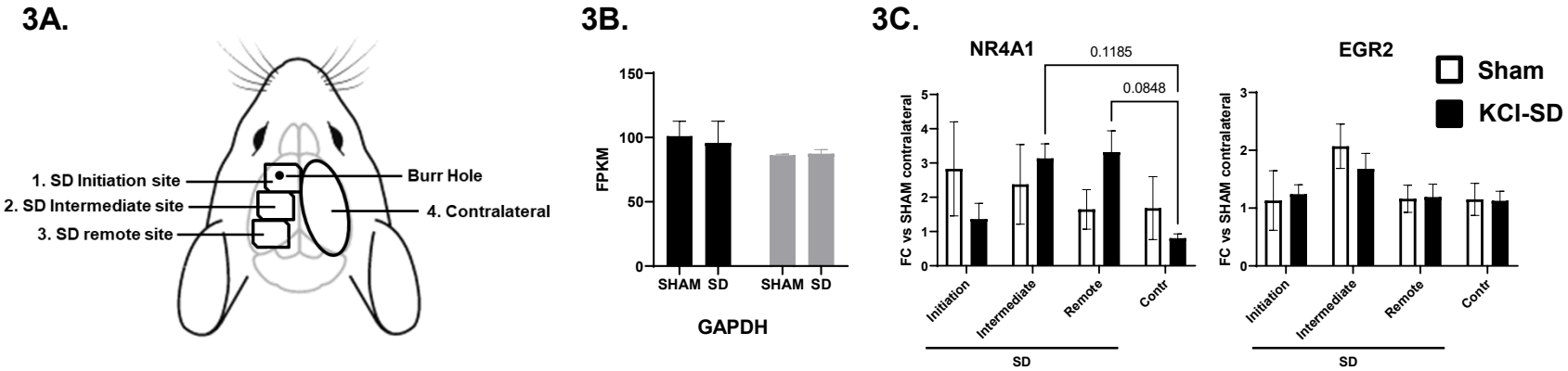
3A.
1. SD Initiation site
2. SD Intermediate site
3. SD remote site
Burr Hole
4. Contralateral
3B.
FPKM
150
100
50
0
SHAM SD SHAM SD
GAPDH
3C.
NR4A1
0.1185
0.0848
FC vs SHAM contralateral
Initiation
Intermediate
Remote
Contr
SD
EGR2
Sham
KCl-SD